

ARTICLE

High resolution data reveal fundamental steps and turns in animal movements

Richard M. Gunner¹  | Rory P. Wilson² | Miguel Lurgi²  | Luca Börger^{2,3} | James Redcliffe² | Emily L. C. Shepard² | Mark D. Holton² | Margaret C. Crofoot^{1,4,5} | Abdulaziz Alagaili⁶ | Samantha Andrzejaczek⁷  | Daniel Ariano-Sánchez^{8,9}  | Thomas Barbedette-Gerard^{2,10} | Nigel C. Bennett¹¹ | Alice Bernard¹² | Rowan Brown¹³ | Nik Cole^{14,15} | Scott Creel¹⁶  | Arioaldo P. Cruz-Neto¹⁷ | Agustina di Virgilio^{18,19} | Carlos M. Duarte²⁰ | Christophe Eizaguirre²¹ | Kyle H. Elliott²² | Monika Faltusova¹⁹ | Mathieu Garel²³ | Natasha Gillies^{24,25} | Adrian C. Gleiss²⁶ | Aoife Göppert²⁷  | David Grémillet^{12,28} | Sophie de Grissac²⁹ | Tim Guilford²⁵ | Maxime Hoareau^{2,10} | Mark Jessopp³⁰ | Agustina Gómez-Laich³¹ | Milos Jezek¹⁹ | Sergio A. Lambertucci^{18,32}  | Pascal Marchand²³  | Nikki Marks²⁷ | Andréia Martins³³ | Mark Meekan^{34,35}  | Yuichi Mizutani³⁶ | Rasmus M. Mortensen^{9,37}  | Bradley M. Norman^{38,39} | Josue Ortega^{1,5} | Oliver Padgett²⁵ | Michael Painter²² | Aurore Ponchon^{12,40}  | Pascal Provost⁴¹ | Aurélien Prudor⁴² | Flavio Quintana⁴³ | Stefanie Reinhardt⁹ | Samantha D. Reynolds^{37,38}  | Frank Rosell⁹ | Carlos R. Ruiz-Miranda⁴⁴  | Peter G. Ryan²⁸ | David M. Scantlebury^{11,27} | Stefan Schoombie²⁸ | Rebecca Scott⁴⁵ | Vaclav Silovsky¹⁹ | Jeroen Steenbeek⁴⁶ | Vikash Tatayah¹⁵ | Carole Toigo²³ | Lucia Torrez^{1,5} | Fred Tremblay²² | Joshua P. Twining⁴⁷  | Ken Yoda³⁶  | Henri Weimerskirch⁴⁸  | Shannon Whelan²²  | Juan M. Morales^{49,50}  | Jonathan R. Potts⁵¹ 

Correspondence

Richard M. Gunner
Email: richard.m.g@hotmail.com

Funding information

The Beveridge Herpetological Trust; The Jock Clough Marine Foundation; Rolex Awards for Enterprise; The European

Abstract

Animal movement paths display substantial complexity and variability, promoting efforts to identify universal rules and models that best describe them. Using high-resolution (≥ 10 Hz) movement from 43 vertebrate species spanning diverse taxa, body sizes, and lifestyles, we show that paths are universally

Richard M. Gunner and Rory P. Wilson contributed equally to this study.

For affiliations refer to page 21

This is an open access article under the terms of the [Creative Commons Attribution](https://creativecommons.org/licenses/by/4.0/) License, which permits use, distribution and reproduction in any medium, provided the original work is properly cited.

© 2026 The Author(s). *Ecological Monographs* published by Wiley Periodicals LLC on behalf of The Ecological Society of America.

Research Council Advanced Grant Program FP7/2007–2013, Grant/Award Number: ERC-2012-ADG_20120314; Alexander von Humboldt-Stiftung; National Science Foundation, Grant/Award Numbers: DEB-2032131, IOS1145749; RAC Parks and Resorts; The MG Kailis Group; Enterprise; Biotechnology and Biological Sciences Research Council (BBSRC), Grant/Award Number: BB/M011224/1; European Union, Grant/Award Numbers: 715874, PICT 2015; Royal Society for the Protection of Birds; NSERC; Norwegian Society of Sciences and Letters Special; European Union's Horizon Europe Research and Innovation Programme, Grant/Award Number: 101060072 (ACTNOW); European Research Council; Challenge Fund and Newry, Mourne and Down District Council; Durrell Conservation Trust; Supporting Project, Grant/Award Number: RSPD2023R602; The Australian Institute of Marine Science, the Japan Society of the Promotion of Science, Grant/Award Numbers: 16H01769, 16H06541, 21H05294, 22H00569; International Association of Avian Trainers & Educators (IAATE); King Saud University; South African National Antarctic Programme; ANCYPT, Grant/Award Number: PICT 2021-I-A-00484; Royal Society/Wolfson Lab; King Abdullah University of Science and Technology (KAUST); Whitley Wildlife Conservation Trust; National Geographic, Grant/Award Number: GEFNE69-13; The Holsworth Wildlife Research Endowment, The UWA Graduate Research School, Grant/Award Numbers: 10.18258/7190, QK1910462; Ministry of Agriculture of the Czech Republic, Grant/Award Number: EVA4.0; Czech University of Life Sciences in Prague, Grant/Award Number: 82/2021; European Regional Development Fund; National Agency for Science Promotion, Grant/Award Numbers: PICT 2017-1996, PICT 2018-01480; First Trust Travel Scholarship at Queen's University Belfast; European Research Executive Agency (REA), Grant/Award Number: 101060072; Ministerio de Ciencia, Tecnología e Innovación Productiva, Argentina; Max Planck Institute for Animal Behaviour's Department for the Ecology of Animal Societies, Grant/Award Number: CP1217; JST CREST, Grant/Award Number: JPMJCR23P2; Wilderness Wildlife Trust, Tusk Trust; The Bennink Foundation, Painted Dog Conservation Inc; World Wildlife Fund; Gemfields Inc; National Geographic Society; IUCN Save Our Species (SOS); OP RDE project Improvement in Quality of the Internal Grant Scheme, Grant/Award Numbers:

composed of straight-line steps interspersed with sharp turns, echoing patterns documented in lower taxa such as bacteria. We report how vertebrate “fundamental steps”—straight travel segments between successive detected turns (with $F_{\text{stepduration}}$ as the turn-to-turn interval and $F_{\text{steplength}}$ as the corresponding distance when displacement is available)—and “fundamental turn angles” ($F_{\text{turnangles}}$; net changes in travel heading between successive steps) vary with species' mass, locomotor mode, behavior, and environment. Here, “fundamental” denotes the finest scale step/turn events resolvable under our sampling rate and turn-detection criteria; these event-scale steps/turns are intrinsically different from the straight-line segments inferred from low-resolution position data. To explain these relationships, we posit that animals inherently move in a straight line until sensory information signals a better heading, triggering a turn. Across all species examined, animals spent the vast majority of their travel time moving in straight lines (species-level means >90%), with turns representing discrete decision points influenced by body size, locomotor mode, and ecological context. Larger animals turned less frequently, consistent with biomechanical constraints of mass and rotational inertia, while aerial species often exhibited higher turning rates driven by soaring flight demands. We further show that turns can be linked to diverse behavioral drivers, including prey pursuit, obstacle avoidance, predator evasion, and exploitation of environmental energy. By explicitly quantifying turns, we clarify how distributions of step durations and turn angles interact to shape movement patterns and why different statistical models (e.g., correlated random walks, Lévy flights) emerge when lower resolution data are analyzed. Finally, we demonstrate how fundamental steps and turns can be incorporated into an agent-based modeling framework using penguins as a case study, enabling reconstruction of realistic tracks and prediction of movement responses to environmental change. Straight-line travel punctuated by decision-driven turns thus emerges as a fundamental principle of vertebrate movement, linking fine-scale movement structure, ecological context, and emergent patterns of space use.

KEYWORDS

accelerometer, agent-based model, animal movement, bio-logging, dead-reckoning, heading, magnetometer, step length, turn angle, turning points

CZ,02.2.69/0.0/0.0/19_073/0016944,
CZ,02.1.01/0.0/0.0/16_019/0000803

Handling Editor: Andrew B. Davies

INTRODUCTION

The routes that self-propelled animals take as they move around their environment have fascinated and perplexed people for centuries (Fernandez, 2014). Understanding the drivers and rules behind animal path complexity and variability across scales remains a major challenge, particularly in vertebrates (Hooten et al., 2017; Nathan et al., 2008). In recent decades, however, advances in animal-borne telemetry have begun to address this challenge, making it possible to quantify the movement of free-living vertebrates (Kays et al., 2015), and providing a foundation for mathematical descriptions and models of movement. The underlying processes that generate observed animal movement paths can be conceptualized in discrete or continuous time (Calabrese et al., 2016; Gurarie et al., 2017; Johnson et al., 2008; McClintock et al., 2014; Nathan et al., 2022). Continuous-time movement models (CTMMs) address key limitations of step-based analyses by treating relocations as observations from an underlying continuous-time stochastic process, accommodating irregular sampling schedules and location error (Calabrese et al., 2016; Fleming et al., 2020). In frameworks such as CTMM, characteristic autocorrelation time scales can be estimated and used for robust inference on movement and space use without imposing a fixed sampling interval (Noonan et al., 2019), making CTMMs a widely used remedy for coarse, duty-cycled, or irregular GPS schedules (Calabrese et al., 2021). However, because they are driven by positional observations, the fine-scale sequence of reorientations between fixes remains latent, motivating complementary approaches that observe directional change directly.

The most common approach for describing animal trajectories uses straight lines to link locations acquired at relatively large sampling intervals (e.g., minutes to hours), generating movement “steps,” with corresponding turn angles between them (Turchin, 1998). This has produced observations and theories that form the bedrock of much of quantitative animal movement ecology (Turchin, 1998). Nonetheless, such step lengths and turn angles remain an approximation of the true movement path and, lacking the necessary temporal resolution, it is unclear how true animal paths are structured (Munden et al., 2021).

In practice, this limitation stems from how movement is typically measured. Most large-scale tracking relies on satellite or GPS telemetry that provides absolute locations

but often at relatively coarse intervals due to battery constraints, duty cycling, and tag size/mass limits (Dewhurst et al., 2016). Moreover, fix success and location error can be strongly habitat- and context-dependent, degrading under dense canopy or rugged terrain, failing entirely underground (e.g., fossorial or cave-using species), and being unavailable during submergence for diving taxa (Costa et al., 2010; DeCesare et al., 2005; Redcliffe, Boulerice, et al., 2025). Even when high fix rates are available, meter-scale location error can obscure fine-scale heading changes when displacement between fixes is small, biasing inference on tortuosity and turn frequency (Gunner et al., 2022; Hurford, 2009). As a result, “steps” and “turn angles” are commonly inferred from straight lines drawn between temporally separated fixes, so that multiple reorientations can be aliased into a single step as sampling intervals increase. By contrast, high-frequency magnetometer-derived heading can provide a complementary stream of information by observing directional change directly at the time scale at which it occurs (Gunner, Holton, Scantlebury, van Schalkwyk, et al., 2021), allowing the geometry of movement to be described in terms of event-based turns rather than fix-to-fix steps. Specifically, animal-borne inertial sensors (accelerometers and magnetometers) can sample at tens of hertz and provide continuous information on body motion and heading; when magnetometry is combined with accelerometry for tilt compensation, heading can be resolved at sub-second scales (Bidder et al., 2015; Gunner, Holton, Scantlebury, van Schalkwyk, et al., 2021). This creates an opportunity to quantify path geometry at a resolution where changes in direction are directly observed rather than inferred from sparse positions.

In his seminal work on animal movement, Turchin (1998) notes that “many organisms tend to move relatively straight for a period of time, and then make a turn and move in another direction.” He illustrates this primarily with prokaryotes and invertebrates, although he gives an example from a bird. Turchin’s observations have been more recently linked to fundamental principles of physics and behavioral ecology: Straight-line travel is energetically and cognitively efficient because it minimizes the mechanical work required to overcome inertia (Brown et al., 2021), avoids the muscular effort involved in initiating and completing a turn, and reduces the need for constant sensory processing and decision-making (Biewener & Daley, 2007). In contrast, turning demands active neuromuscular control

(Biewener & Daley, 2007), elevated energy expenditure to redirect momentum (Wilson et al., 2013; Wilson, Rose, Metcalfe, et al., 2021), and engagement of cognitive processes (Hills, 2006; Plass et al., 2010) to evaluate new sensory input and determine an appropriate new heading (Kashetsky et al., 2021). Consequently, animals should theoretically favor straight-line travel unless ecological or environmental stimuli necessitate directional changes. Building on this previous understanding, we hypothesize that animal movement consists predominantly of straight-line sections interspersed with discrete turning events.

To test our hypothesis, we used high-resolution bio-logging technology—specifically magnetometers and accelerometers—to quantify true movement paths in 43 vertebrate species using sub-second measurements of heading (≥ 10 Hz). While GPS can quantify displacement between fixes, high-frequency heading allows us to detect turning behavior at the time scale at which it occurs, including fine-scale reorientations that are easily aliased into straight steps at common GPS sampling intervals. Where absolute positions were required for case studies, we used GPS-corrected dead-reckoning to reconstruct paths between fixes, combining the strengths of inertial and positional telemetry (Gunner, Holton, Scantlebury, Hopkins, et al., 2021). Together, these advances allow us to evaluate whether the straight-line/turning structure that has been assumed in movement ecology is evident in near-continuously observed movement paths. Our study encompassed a diverse array of taxa, including fish, reptiles, birds, and mammals, spanning a wide range of habitats across the globe and body sizes from 0.3 to over 10,000 kg. We first assessed how sampling frequency influences the characterization of movement paths, with particular focus on the extent to which these paths can be described as sequences of straight-line segments punctuated by discrete turns. We then evaluated how path geometry, described in terms of step lengths and turn angles, varies across species, and explored potential associations with functional traits such as body size, locomotory medium, and lifestyle. Finally, we considered how this approach might refine models of space use and offer new perspectives on how animals perceive and engage with their environments.

METHODS

Tag deployment details and analysis

We deployed Daily Diary (DD) tags (Wilson et al., 2008) on 43 species (15 birds, 3 fish, 3 reptiles, and 22 mammals) covering a size range of 0.3–10,000 kg to obtain

data on their movement patterns. The tags contained tri-axial magnetometers, tri-axial accelerometers, and pressure sensors (Wilson et al., 2008), allowing travel headings over time to be deduced (Gunner, Holton, Scantlebury, van Schalkwyk, et al., 2021). Sampling rates ranged from 10 to 40 Hz, and derived tracks were subsampled to either 10 or 20 Hz for analysis. See Appendix S1: Table S1 for detailed information on sampling rates, sample size, locations, and deployment dates. Refer to Appendix S1: Section S1 for ethical approvals, funding sources, and acknowledgments pertaining to each species.

Tag data were first processed to exclude periods immediately following the tagging process to minimize the probability of potential tagging effects; this exclusion period typically lasted a few days. Data were then examined to identify extended periods of active movement (excluding non-traveling movement behavior), noting the travel medium: air, water, or on land. From these periods, a single continuous segment (usually between 5 and 36 h) was analyzed per individual animal. The variation in duration was entirely due to the variation in activity patterns among species. For example, pine martens were typically only continuously active for a few hours a day, whereas sharks swam continuously. The compass and acceleration data were used to calculate headings following methods described in Gunner, Holton, Scantlebury, van Schalkwyk, et al. (2021). Additionally, for select case studies, absolute animal locations over time were determined via dead-reckoning, incorporating periodic verified locations obtained through co-deployed GPS to correct for drift (Gunner, Holton, Scantlebury, Hopkins, et al., 2021). In these instances, step lengths could be used to quantify movement patterns. Step lengths can be interpreted as the integral of speed over each step duration, while turn angles quantify changes in movement direction between successive steps.

Variations in turns within the heading data were identified using the protocol defined by Potts et al. (2018). These variations ranged from an average minimum of 10 turns per hour across individuals for whale sharks to an average maximum of 207 turns per hour for the European pine marten. Briefly, the algorithm detects changes in the heading by sliding a small window across the time series of headings and calculating the squared circular standard deviation (SCSD) within the window. Spikes in SCSD indicate turns, and candidate turns were filtered based on achieving a threshold turn angle of 30° for all species (Munden et al., 2021; Potts et al., 2018) within a species-specific time window (see Potts et al. (2018) and Appendix S1: Section S2 for details). We define a “fundamental step” as the interval between successive detected turning points (a turn-to-turn segment)

during which travel heading is approximately stable; $F_{\text{stepduration}}$ is the elapsed time of this interval. Where speed or dead-reckoned displacement is available, $F_{\text{steplength}}$ is the distance traveled during the same interval. Each detected turning point yields a fundamental turn angle ($F_{\text{turnangle}}$), defined as the net change in travel heading between successive steps. To quantify the extent to which trajectories can be represented as straight segments punctuated by turns, we classified each segment between successive turning points as “straight-line travel” when its within-segment normalized deviation from a straight line (e_k ; dimensionless; Appendix S1: Section S2) fell below a threshold $e_{\text{thresh}} = 0.1$ (10%). This threshold affects the *proportion* of movement classified as straight, but it does not affect the identification of turning points from the heading time series.

Mass-scaling analysis

For each locomotion mode $m \in \{\text{terrestrial, aerial, aquatic}\}$, we modeled the species-level mean of $\ln(F_{\text{stepduration}})$ of body mass using ordinary least squares (OLS):

$$\underbrace{\overline{\ln(T_{im})}}_{Y_{im}} = \alpha_m + s_m \times \log_{10}(M_i) + \epsilon_{im},$$

where i indexes species, T is fundamental step duration (in seconds), $Y_{im} = \ln(T_{im})$ is the species-level mean of the natural log of fundamental step duration ($\ln(F_{\text{stepduration}})$), that is, the log of the geometric mean step duration; M_i is species-typical body mass (in kilograms), α_m is the intercept, s_m the slope, and ϵ_{im} the residual.

Because $\log_{10}M = (\ln M)/\ln 10$, the slope s_m corresponds to a power-law exponent $b_m = s_m/\ln 10$, so that on the original scale, the geometric mean step duration follows

$$\exp(\overline{\ln T}) = e^{\alpha_m} M^{b_m},$$

and equivalently, $\log_{10}\{\exp(\overline{\ln T})\} = \alpha'_m + b_m \log_{10}M$, with $\alpha'_m = \alpha_m/\ln 10$. We report b_m with 95% CIs obtained by transforming the slope CI:

$$\text{CI}(b_m) = (s_m \pm 1.96 \text{SE}(s_m))/\ln 10.$$

Model diagnostics

For each locomotion mode, we assessed standard OLS assumptions. Linearity was evaluated with component-plus-residual plots and by adding a quadratic term $\log_{10}(M)^2$ (likelihood-ratio test [LRT] and difference in Akaike information criterion between models [ΔAIC]). Homoscedasticity was examined via residuals-versus-fitted plots and Breusch–Pagan tests. Residual normality

was inspected using Q–Q plots; formal tests are low power at species-level n . Influence was assessed using Cook’s distance (flagging points with $D_i > 4/n$) and leverage. As robustness checks, we computed heteroscedasticity-consistent (HC3) standard errors and, where species-level ln-means had available standard errors, fitted weighted least squares with inverse-variance weights. In all three locomotion modes the quadratic term was not supported (LRT $p = 0.194$ terrestrial, 0.515 aquatic, 0.150 aerial; $|\Delta\text{AIC}| \leq 1.01$). Breusch–Pagan tests indicated adequate homoscedasticity (terrestrial $p = 0.537$, aerial $p = 0.564$); aquatic was borderline ($p = 0.076$), but HC3 standard errors led to the same substantive inference. Three terrestrial and one aquatic species exceeded the Cook’s $4/n$ heuristic; refits excluding these points yielded essentially unchanged slopes and conclusions.

Sensitivity to body mass uncertainty

To evaluate whether uncertainty in species-typical body masses could influence the estimated scaling relationships, we performed a Monte Carlo sensitivity analysis in which we perturbed $\log_{10}(M)$ using mean-zero Gaussian noise corresponding to plausible coefficients of variation in mass (10%–30%) and refit the OLS models (5000 simulations per locomotion mode). The resulting distributions of slopes s_m (and derived exponents b_m) were very similar to the original estimates in all three locomotion modes. Across 10%–30% mass CV, median slopes s_m (on $\log_{10}(M)$ in the ln-response model) changed only slightly (e.g., terrestrial $s_m = 0.233 \rightarrow 0.229$; aquatic $s_m = 0.313 \rightarrow 0.311$; aerial $s_m = 0.143 \rightarrow 0.134$), with wider uncertainty only under the most conservative error assumptions for aerial species.

Agent-based modeling

We developed an agent-based model to predict the movement paths of Magellanic penguins (*Spheniscus magellanicus*) foraging at sea by utilizing empirical data from GPS-corrected dead-reckoned tracks of 27 individuals, including fundamental step length ($F_{\text{steplength}}$), turn angle ($F_{\text{turnangle}}$), and associated compass heading (H). The foraging landscape was divided into equally spaced grid cells of area 10 km², enabling the calculation of unique frequency distributions (empirical cumulative distribution functions, ECDFs) for $F_{\text{steplength}}$, $F_{\text{turnangle}}$, and H within each grid cell. These distributions were further segmented by journey phase, defined as either outbound or inbound. The transition from outbound to inbound was identified by the onset of a continuous downward

gradient in the penguins' cumulative shortest distance to the colony. At the beginning of the simulation, each agent's movement parameters ($F_{\text{steplength}}$, $F_{\text{turnangle}}$, and H) were initialized based on the outbound ECDF distributions from the grid cell corresponding to their departure point near the colony. Each agent navigated a virtual 2D spherical coordinate system. At each time step, $F_{\text{steplength}}$ and $F_{\text{turnangle}}$ were randomly drawn from their respective ECDFs, and the direction of each turn was selected to align with the sampled H . At each movement step, the agent was dead-reckoned using this information to recalculate its geographical position and cumulative (Haversine) distance traveled. Upon entering a new grid cell, the agent recalibrated its $F_{\text{steplength}}$, $F_{\text{turnangle}}$, and H distributions using the ECDF data specific to that grid cell. When the cumulative distance reached a user-defined proportion of the maximum distance threshold, the agent updated its grid cell ECDF information to reflect the inbound phase of the foraging trip. The simulation continued until each agent had traversed a user-defined total cumulative distance traveled.

RESULTS AND DISCUSSION

The case for straight lines and turns

Key to our analysis is the temporal resolution of animal heading, derived from onboard magnetometers (Gunner, Holton, Scantlebury, van Schalkwyk, et al., 2021), which, at 20 Hz (except for two species at 10 Hz, see Appendix S1: Table S1), precludes the possibility of changes in trajectory going undetected. Such data offer an essentially continuous representation of animal movement, a stark contrast to the traditional method that determines step lengths from sparsely spaced locations—usually once every 5 min to a few hours (Gunner, Holton, Scantlebury, Hopkins, et al., 2021). Under those traditional methods, multiple turns can be simplified into straight lines connecting infrequent, discrete locations, potentially smoothing out important details in the path (Munden et al., 2021). Instead, we used a turn identification protocol (Potts et al., 2018) (for detailed methods see Appendix S1: Section S2) that generally revealed what were visually obvious straight lines and turning points (Figure 1). We suggest that the associated step durations represent a precisely defined travel behavior: maintaining an approximately stable heading between successive detected turns, that is, a movement ecology “step” (not a locomotor step/stride). We term the resulting turn-to-turn elapsed times “fundamental step durations” ($F_{\text{stepdurations}}$). When speed (or dead-reckoned displacement) is available, the corresponding fundamental step length ($F_{\text{steplength}}$) is the distance traveled during that same

interval; accordingly, step durations are not necessarily proportional to the step “lengths” commonly used in location-based studies, although they equate directly if animals travel at constant speed. The angular reorientations associated with detected turning events (i.e., the net change in travel heading between successive steps) are termed “fundamental turn angles” ($F_{\text{turnangles}}$). We use “fundamental” as shorthand for the finest scale step/turn units resolvable at our sampling resolution and turn-detection criteria, not as a claim of universal invariant rules across taxa.

Conceptually, step durations, step lengths, and turn angles are coupled through velocity, because velocity is a vector with both magnitude (speed) and direction. In a continuous-time view, the animal's path can be described by a velocity vector $v(t)$ (Johnson et al., 2008). Our “fundamental steps” correspond to intervals of relatively stable movement direction, whereas “fundamental turns” correspond to reorientations (changes in the direction of $v(t)$). This provides a direct link between step/turn descriptions and continuous-time velocity-based movement models: step lengths arise from integrating speed over each step duration, and turns quantify directional changes between successive velocity headings (Gurarie et al., 2017).

For every species, the species-level mean proportion of movement time traveling in straight lines exceeded 90% (classified using the segment deviation threshold $e_{\text{thresh}} = 0.1$; Appendix S1: Section S2), with 84% (36 out of 43 species) spending >95% in straight-line trajectories (Figure 1). Unsurprisingly, sections defined as “straight line” were usually not perfectly straight (Turchin, 1998) and followed one of two fundamental patterns of wobble (where we define “wobble” as the ratio between the mean deviation of a path segment from a straight line and the length of that line— e_k in Appendix S1: Section S2: Equation S4). There was a “general baseline wobble” in most species, such as that displayed by the Eurasian beaver, *Castor fiber* (Figure 1D), or the particular case of “systematic wobble” in many procellariiform species, notably albatrosses, which manifested as a long, flat, sine wave-type pattern across 2D space (Figure 1E). This is due to their dynamic soaring flight, which requires this pattern to extract energy from the wind and waves to minimize costs of transport (Kempton et al., 2022). In both wobble types, none of the species exhibited a mean wobble value above 0.05. Across all species, the mean wobble value was 0.019 ± 0.009 (± 1 SD), although there was appreciable variation between species (Figure 1F). Thus, describing the paths between identified turning points as a straight line provided a good approximation to all observed tracks. The “general baseline wobble” is presumably due to minimal navigational errors as well as animals being marginally affected by conditions *en route*, such as gusts of wind for flying birds

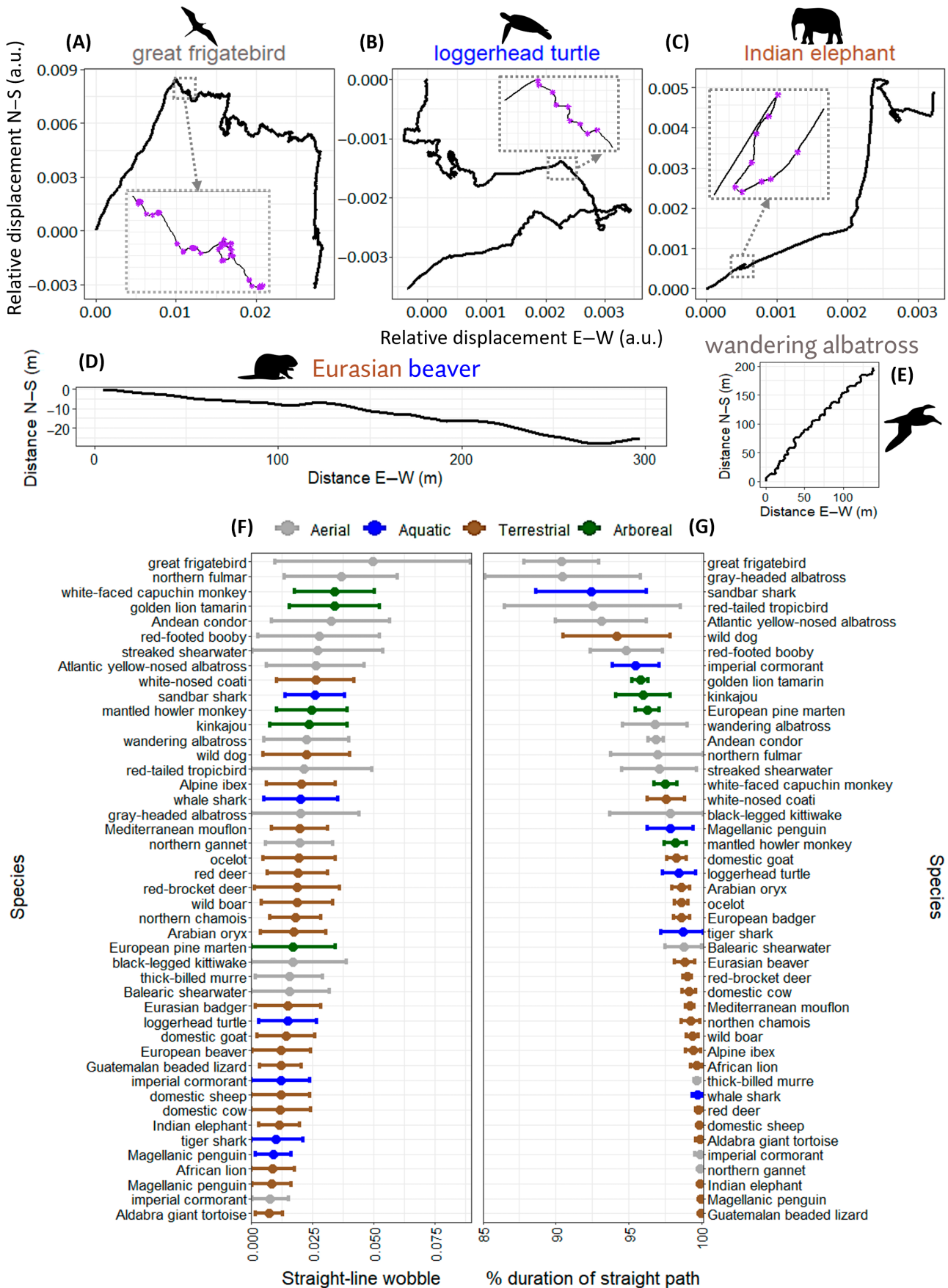


FIGURE 1 Legend on next page.

or minor changes in substrate or topography for terrestrial animals (Shepard et al., 2013).

Straight-line features are influenced by species traits and environments

$F_{\text{stepdurations}}$ varied substantially within and between species, but frequency distributions were all right-skewed and unimodal, even when viewed on a log scale (Figure 2A). Mean $F_{\text{stepduration}}$ varied between 12 s (European pine marten, *Martes martes*) and 54 s (whale shark, *Rhincodon typus*), and were species-specific (Figure 2B). Mean $F_{\text{stepduration}}$ increased with animal mass except for aerial species (Figure 2C): Linear models (see *Methods*) revealed strong and significant positive relationships for terrestrial (intercept = 2.608, slope on log10 mass $s_m = 0.234$; exponent $b_m = 0.102$, 95% CI = 0.054–0.149, $R^2 = 0.458$, $p < 0.001$) and aquatic species (intercept = 2.738, $s_m = 0.314$, $b_m = 0.136$, 95% CI = 0.039–0.233, $R^2 = 0.791$, $p = 0.018$) but no relationship for aerial species (intercept = 2.885, $s_m = 0.144$, $b_m = 0.062$, 95% CI = -0.208–0.333, $R^2 = 0.021$, $p = 0.625$).

Importantly, the relationship between step durations and turning rates (rate = 1/duration) meant that turning rates were higher in small terrestrial and aquatic species. One possible explanation for the observed scaling relationship is that large animals experience greater inertial constraints due to increased body mass and rotational inertia, making directional changes disproportionately energetically costly. According to fundamental biomechanical principles, rotational inertia scales approximately with the mass and dimensions of an animal, meaning that large animals must generate substantially greater muscle forces and higher torque to achieve the same angular acceleration during directional changes (Alexander, 2003; Domenici, 2001). This biomechanical relationship explains

why large species often exhibit lower maneuverability than small species, as demonstrated by comparative studies of terrestrial mammals and aquatic vertebrates (Domenici, 2001; Wilson et al., 2015). Consequently, large animals may preferentially adopt movement strategies that reduce the frequency or magnitude of directional changes, aligning with the energetic optimization observed across diverse taxa (Weihs & Webb, 1984; Wilson et al., 2013).

The mass-scaling exponents for fundamental step duration, which inversely relates to turning rates, are comparatively shallow (≈ 0.10 – 0.14 ; Figure 2C) relative to some classic biomechanical scalings (e.g., stride length $\sim M^{0.33}$; characteristic limb/wing cycle times $\sim M^{0.33}$; preferred terrestrial speed $\sim M^{0.17}$). One hypothesis is that larger animals require stronger sensory cues to initiate turns because maneuvering has higher energetic/inertial costs (Appendix S1: Section S3), yielding longer steps (lower turn frequency). That said, the variation in step duration across ~ 5 orders of magnitude in body mass is relatively modest (Figure 2B), so this mechanism should be viewed as hypothesis-generating rather than definitive. The absence of a mass trend in flying birds likely reflects our sample being dominated by soaring species >1.5 kg, which execute frequent course corrections to exploit thermal or dynamic soaring (Williams, Shepard, et al., 2020); inclusion of large obligate flapping bird species such as geese may alter this outcome.

The identification of turns is important because they are not only energetically costly (Voigt & Holderied, 2012; Wilson et al., 2013; Wilson, Rose, Metcalfe, et al., 2021), but fundamental turns could represent decision points, where specific inputs have elicited a change in heading (Gunner et al., 2023; Munden et al., 2021) resulting in movement to a different environmental space than if the animal had not turned. Specifically, animals can incur the energetic costs of turning because the likely fitness benefits of turning outweigh

FIGURE 1 Vertebrate movement paths are primarily composed of straight-line sections. (A–C) Examples of dead-reckoned (not GPS-corrected) movement trajectories reconstructed using data (>5 h) from species with different lifestyles and using the lifestyle indicated when the data were taken; aerial (great frigatebird, *Fregata minor*), aquatic (loggerhead turtle, *Caretta caretta*), and terrestrial (Indian elephant, *Elephas maximus indicus*). Axes show relative displacement (a.u.) from the start point (0,0); absolute position, orientation, and scale are arbitrary. Identified turn points are shown in the inserts as purple stars. (D and E) Minor deviations in path segments (wobble), defined nonetheless as straight-line, from a Eurasian beaver, *Castor fiber*, and a wandering albatross, *Diomedea exulans*, respectively, where the former illustrates general wobble, while the latter is due to the sinusoidal movement that procellariiforms use during dynamic soaring—plotted in meters where calibration is available. (F) Mean (± 1 SD) straight-line wobble (for calculations see Appendix S1: Section S2) of our study species and (G) mean percentage of the total path duration that is estimated to be straight-line travel (defined as having an average deviation of less than 10% from a straight line—see Appendix S1: Section S2). The color coding of species in the last two figures is based on their dominant mode of locomotion/lifestyle (gray = aerial, blue = aquatic, brown = terrestrial, green = arboreal). Note, however, there are exceptions in certain cases. For example, data for the Eurasian beaver, *Castor fiber*, encompassed both terrestrial and aquatic movement, white-nosed coatis, *Nasua narica*, occasionally engage in arboreal movement, and the data for Magellanic penguins, *Spheniscus magellanicus*, and imperial cormorants, *Leucocarbo atriceps*, were divided into aquatic and terrestrial phases (for the former), and aerial and aquatic phases (for the latter) stages, each of which was analyzed independently. Silhouette illustrations credit: Imran Razik.

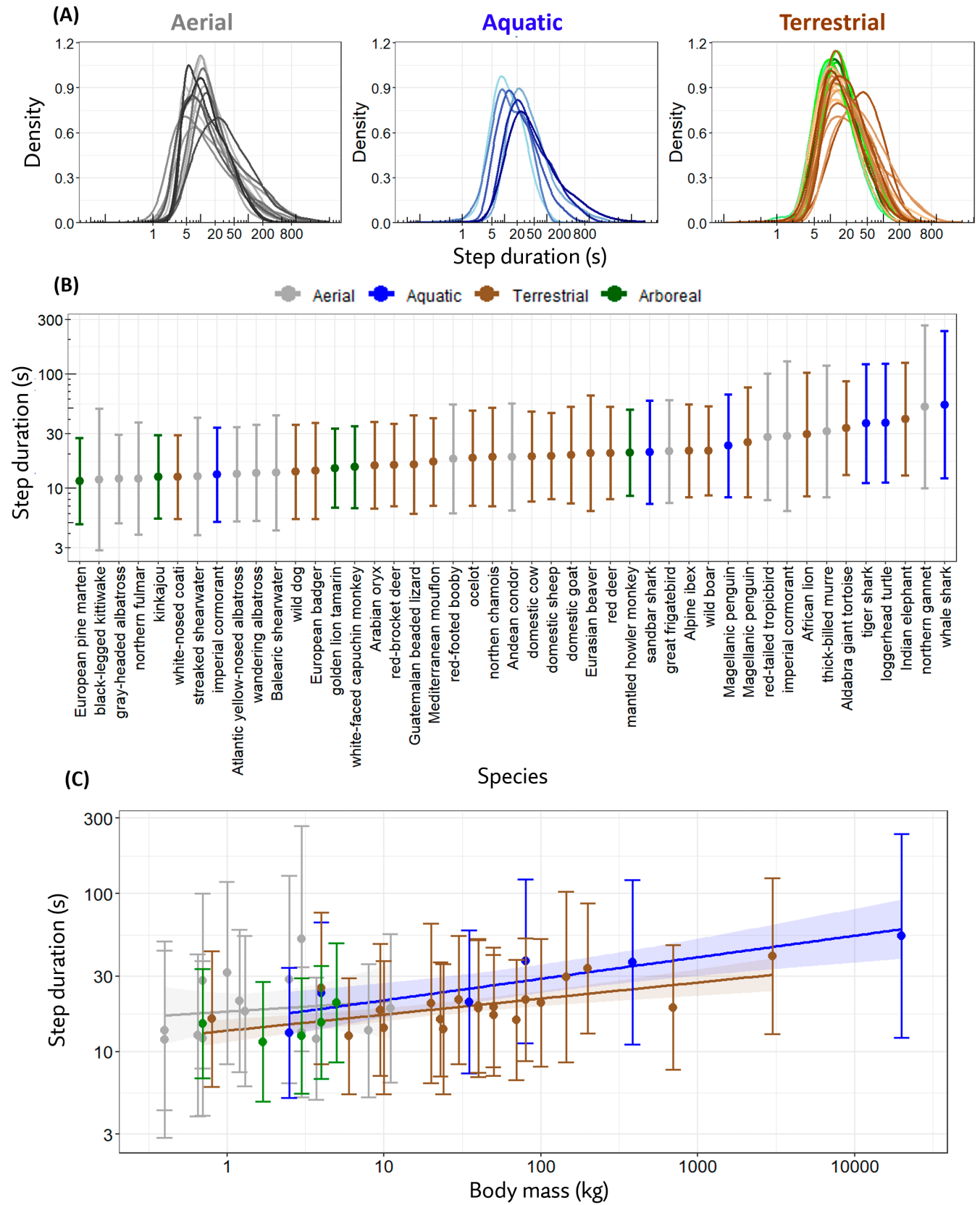


FIGURE 2 Legend on next page.

those of continuing in a straight line. Laboratory maze work tells us that paths taken are driven by animal choice at every turn (Bailey et al., 2021). Similarly, animals free to move in two or three dimensions, from insects to sharks, follow odor plumes to their source, altering heading in relation to changing odor density (Vickers, 2000). Wild birds follow tactile and visual cues over mm and km scales, respectively (Nolet & Mooij, 2002). This highlights the value of identifying true turns, as it means that there is potential to link them to environmental predictors over different scales, recognizing that the way animals respond to perceived cues (including social information; Dall et al., 2005) will be modulated by past experiences and their internal state such as changing levels of hunger (Nathan et al., 2008).

The value of identifying turns is not just applicable to locating resources per se. Although a small proportion of turns may occur due to “spontaneous behavior” such as play (Proekt et al., 2012), we expect many turns to occur when animals move around obstacles in cluttered environments, change heading to exploit sources of environmental energy (such as birds in thermals; Williams, Shepard, et al., 2020), and during escape maneuvers from predators (Wilson et al., 2015). Indeed, not only do obstacles induce turns, but they can also dictate prolonged straight-line movement. For instance, the presence of barriers like fences, walls, roads, and streams can constrain animals to travel “along” them until they encounter a break, permitting a turn. These confounding factors may tend to weaken relationships between turn angle and animal mass because the spatial distribution of environmental cues (e.g., the location of obstacles or food) that elicit (or prevent) turns is not expected to be animal mass-dependent. This, together with the wide variety of behaviors that the movement data encompasses, could contribute to the variability in the relationship between $F_{\text{turnangle}}$ and mass (see also Appendix S1: Table S3).

A simple rule-based framework for interpreting animal movement

Based on our empirical observations, we propose a simple framework to explain animal movement. When an

animal initiates a particular behavior such as foraging, often driven by internal states such as hunger (Morales et al., 2010; Nathan et al., 2008), it adopts a straight-line heading toward what it perceives as the most likely location of its proximate goal (Nathan et al., 2008). This strategy not only reflects the animal’s best estimate based on available information but also minimizes the distance traveled and energy expended between successive decision points. It then proceeds in a straight line along this heading while continuously sampling environmental cues and other sources of information, including the presence of physical obstacles, conspecifics, or other species (Dorfman et al., 2022; Goodale et al., 2010). Changes in direction may also be influenced by memory, triggered by familiar environmental features (Fagan et al., 2013) or shifts in internal state (Nathan et al., 2008). Once a new heading appears more favorable, the animal turns and the process repeats.

Because different behaviors rely on different sensory inputs (e.g., foraging versus returning to a central place), we expect each movement behavior to produce characteristic distributions of $F_{\text{stepdurations}}$ and $F_{\text{turnangles}}$. In general, moving in a straight line from the current position to the next best perceived location is optimal, as it minimizes both distance and energy expenditure (notwithstanding exceptions such as soaring birds using thermals).

Although turns incur additional cognitive and energetic costs, they remain an integral part of efficient movement. We propose that animals incorporate them strategically in response to environmental heterogeneity. This heterogeneity may arise from various sources, including the presence and distribution of obstacles, predators, or resources, and is perceived via diverse sensory modalities. Such turn-eliciting stimuli structure the path and reflect the animal’s ongoing interaction with its environment.

Our work provides empirical evidence to demonstrate that Turchin’s (1998) premise, that “many organisms tend to move relatively straight for a period of time, and then make a turn and move in another direction,” holds for all the vertebrates we examined, covering fish, reptiles, mammals, and birds. This framework is fundamentally different from classic movement models because, instead of incorporating random elements as a

FIGURE 2 Fundamental step durations vary with lifestyle and animal mass. (A) Frequency distributions of $\ln(\text{step duration})$ for all species, colored according to their dominant mode of locomotion; aerial, aquatic, or terrestrial (arboreal species are combined with terrestrial species in panel A). Distinct shades of each color represent different species. (B) Species-level geometric mean $F_{\text{stepduration}}$ by species and lifestyle/locomotion mode (mean \pm 1 SD). (C) Relationship between species-level geometric $F_{\text{stepduration}}$ and body mass across different lifestyle/travel mode on \log_{10} – \log_{10} axes (mean \pm 1 SD). Arboreal species (green) are shown separately for visualization but pooled with terrestrial species (brown) for the regression due to limited arboreal sample size (see Appendix S1: Table S1). Regression fits are from models of $\ln(F_{\text{stepduration}})$ versus $\log_{10}(\text{body mass})$: $\ln(T) = \alpha_m + s_m \times \log_{10}(M)$, which implies the power-law scaling $T = e^{\alpha_m} M^{b_m}$ with $b_m = s_m / \ln(10)$ (see *Methods*).

convenience (Bartumeus et al., 2005), it ascribes path changes to choices based on external cues (or state changes), which may serve as attractors or repellers (of variable importance) (Gunner et al., 2023; Mueller & Fagan, 2008). The range over which diverse animal sensory systems operate, even within one species (Nathan et al., 2008), and the distribution of available cues over space and time is what determines the overall path structure via step lengths that are curtailed by the animals' responses to these cues.

This approach provides a precise framework for analyzing the formulation of animal movement paths, highlighting how even minor changes in turning angles can exert a substantial influence on subsequent space use. While decision-based movement may, over long time periods and with sufficient data, produce statistical signatures that resemble diffusive processes (e.g., mean squared displacement scaling with time), superficially similar metrics can arise from markedly different underlying trajectories. For instance, individual random walks governed by identical stochastic rules may diverge dramatically in their realized paths. Likewise, distinct animals may exhibit patterns consistent with diffusive or even super-diffusive dynamics over extended durations. However, such coarse-grained summaries offer limited insight into the fine-scale structure of movement, the specific locations visited, or the behavioral drivers of path variation. In contrast, treating key inflection points, sharp changes in heading, as behavioral decisions promote a more detailed examination of movement patterns both preceding and following such turns. This perspective can help illuminate the motivational context or urgency behind particular directional shifts. For example, a predator such as a cormorant, which forages underwater, may abruptly alter its trajectory upon detecting pelagic prey (e.g., Appendix S1: Figure S6).

It would be naïve to expect to be able to infer the reasons for all turns in our data due to the large number of cues appealing to diverse sensory systems that might elicit an animal to turn. However, some cases appear clear, including, but not limited to: (1) animals that turn to extract energy from a positive energy landscape (Shepard et al., 2013) (Figure 3A); (2) animals faced with an obstacle that hinders or blocks movement (Figure 3B); (3) turns made by arboreal animals that have to choose between alternative branches in a manner analogous to rats in a maze (Figure 3C); (4) species that use area-restricted search (Barraquand & Benhamou, 2008) to exploit patchy prey changing from “searching” to “exploiting” behavior (Dorfman et al., 2022; Kareiva & Odell, 1987; Weimerskirch et al., 2007) (Figure 3D); (5) animals that turn to reduce overall power requirements for movement in energetically onerous terrain (Figure 3E);

and (6) animals pursued by predators that execute acute, fast turns to enhance their chances of escape (Wilson et al., 2015) (Figure 3F). As part of this, we expect $F_{\text{turnangles}}$ and $F_{\text{stepduration}}$ (or $F_{\text{turnfrequency}}$) to change over space as environmental context changes (Figure 3G), and these may also be different for animals moving in groups.

Importantly, being able to observe $F_{\text{stepdurations}}$ and $F_{\text{turnangles}}$ means that we have access to the true points at which animals alter their paths, which is a first step to recognizing turn elicitors (Figure 3A–F) and a critically important part of understanding what structures animal paths. This makes a case for plotting turn points in space to help understand how movement patterns relate to the environment, which we consider to be a key aspect of studying animal behavior, ecology, and conservation (Mueller & Fagan, 2008). Spatial clustering of particular step lengths is already commonly used, for example, to identify likely feeding areas, associated with area-restricted search behavior (ARS) (Kareiva & Odell, 1987). Georeferencing $F_{\text{turnangles}}$ goes beyond this, allowing scientists to attempt to link true turn points to specific and potentially fine-scale cues (e.g., Figure 3G) (see below).

Frequency distributions of $F_{\text{turnangles}}$ and their relationship to $F_{\text{stepdurations}}$

We found that the distribution of absolute turning angles (i.e., the magnitude of the angle, disregarding whether it is a left or right turn) roughly follows a gamma distribution, truncated at 180° (Appendix S1: Table S4, Figure S5). While this is perhaps an unusual choice of distribution for turning angles, none of the standard distributions (e.g., von Mises, wrapped Cauchy) quite capture the lower probability density close to zero degrees. Although we use a 30° criterion to operationally distinguish turns from fine-scale wobble, estimated turn angles can still fall below this value with nonzero probability due to discretization and measurement noise, so a hard-truncation at 30° is inappropriate (Potts et al., 2018). When turning angles are derived from locations at typical constant sampling frequencies (Munden et al., 2021), the distribution is much closer to a uniform distribution (Figure 4A,B). This indicates a fundamental difference between quantifying animal movement based on $F_{\text{turnangles}}$ from high-frequency, continuously sampled data compared to estimates derived from temporally spaced discrete location data (cf. black versus colored lines in Figure 4A). Critically, the configuration of $F_{\text{stepdurations}}$ and $F_{\text{turnangles}}$ over space and time according to behavior should influence how well different models of animal movement fit lower resolution data. In support of this, we note how many fish have best fit models of

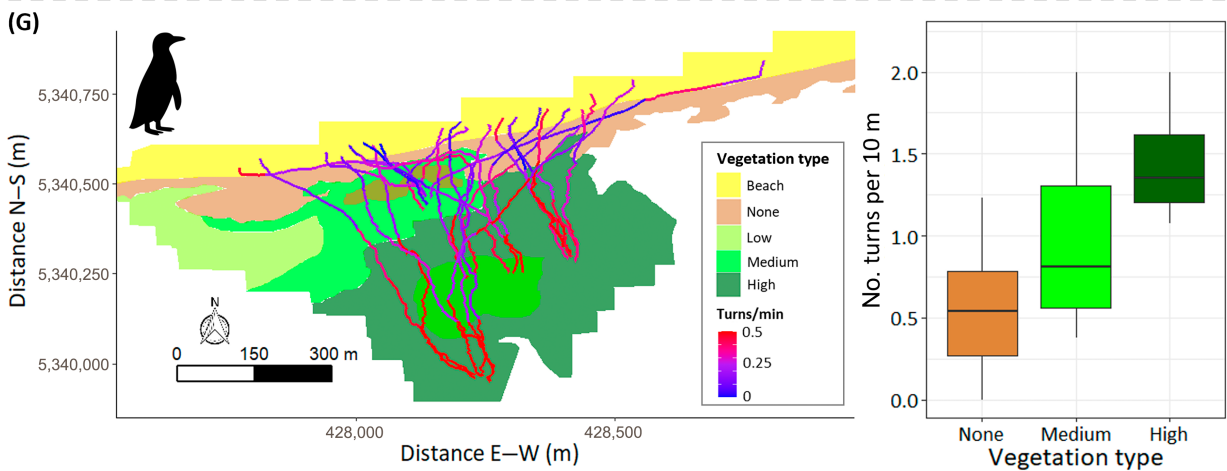
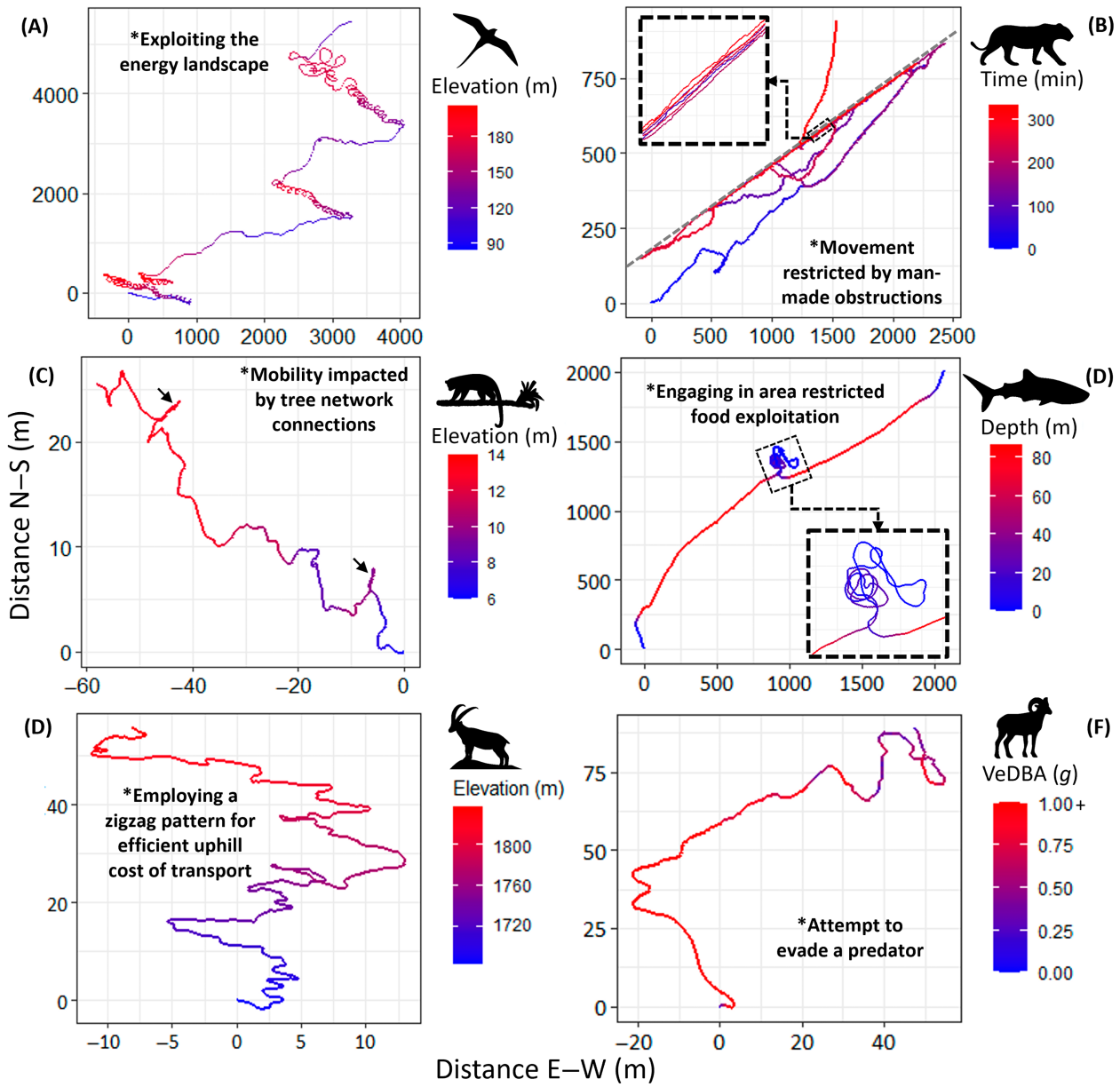


FIGURE 3 Legend on next page.

movement that are best classified by either Brownian or Lévy depending on environmental context, including species that shift their apparent search strategy (and thus the best fitting model: Brownian vs. Lévy) as they move across habitats (Humphries et al., 2010).

Figure 4 shows how step and turn statistics change with sampling interval: As the time between location fixes increases, multiple fundamental turns are increasingly aliased into single apparent steps, inflating step lengths and pushing turn-angle distributions toward uniformity (Munden et al., 2021). This means that heavy-tailed or bimodal step-length patterns inferred from sparse locations can, in part, reflect aggregation over multiple decision events rather than distinct movement modes. More generally, because observation error can generate artefactual path geometry (e.g., spurious turning and biased tortuosity; Hurford, 2009), inference from step-based models should be interpreted as describing an observation-scale path, which may differ from the animal's event-scale movement decisions. CTMMs help reduce sensitivity to irregular sampling by fitting movement in continuous time while accounting for location error (Calabrese et al., 2016; Noonan et al., 2019), but they do not directly resolve how many discrete reorientation events occurred between fixes, information that high-frequency heading provides directly.

How turn angles interact with step durations/lengths is important in shaping movement paths, and in a manner similar to that reported for sparse location data (Hodel & Fieberg, 2022), we detected a correlation between $F_{\text{stepdurations}}$ and $F_{\text{turnangles}}$ for many species (73%, Figure 4C,D, Appendix S1: Table S5). The proportion of terrestrial (and arboreal) species with significant correlations (60%) was significantly lower than the combined proportion for aerial (93%) and aquatic (83%) species (95%; $\chi^2 = 4.34$, $p < 0.05$). We suggest this is due to landscape features continually interrupting what would

otherwise be longer straight-line step lengths for terrestrial animals. This would occur much less in aerial or aquatic species, and certainly in our assemblage of species, although it could occur in marine benthic organisms too.

Where correlations between step durations and turn angles do occur, they could be driven by specific behaviors (Hodel & Fieberg, 2022). For example, animals engaged in directed travel should have long step durations and small turn angles. Short step durations and more acute turn angles would, on the other hand, be expected when animals exploit patchy food resources (Hodel & Fieberg, 2022). Since we assume that, at any given moment, animals adopt specific, single behaviors, the distribution of turn angles and step durations should therefore vary over time as animals switch from one behavior to another (Morales et al., 2004). Our data typically show this, with both $F_{\text{stepduration}}$ and $F_{\text{turnangle}}$ distributions changing over time, and consequently space, across species (e.g., Figure 5A).

More generally, many species showed temporally structured turning rather than turning uniformly at random: Their local-in-time turn-angle distributions often became more concentrated for extended periods. Specifically, for 30 species, the local-in-time turning-angle distribution was more often narrower than a uniform distribution (Figure 5B; 95% CIs entirely above the 50% boundary shown by the dashed line; see Appendix S1: Section S2 for detailed methodology), indicating sustained directional persistence over time. At the other extreme, four species showed the opposite pattern, with local-in-time turning-angle distributions more often indistinguishable from (or broader than) uniform (95% CIs entirely below 50%; Figure 5B). These were dominated by arboreal taxa (four of the five arboreal species), consistent with frequent large reorientations imposed by canopy connectivity and route choice in wooded habitats (Harel et al., 2022) (e.g., Figure 3C). The remaining eight species

FIGURE 3 Unveiling the reasons behind turning-point selection in animal paths. Path structures showing turns in animals exhibiting different behaviors according to environmental context. (A) A red-tailed tropicbird, *Phaethon rubricauda*, changing direction to exploit thermals, (B) an African lion, *Panthera leo*, that had its progression constrained by a fence bounding its National Park (the animal moves repeatedly up and down the fence and eventually finds a way through), (C) a climbing kinkajou, *Potos flavus*, moves along a branch until the branch ends with no vegetation allowing it to continue in its preferred direction (about-turn points shown by arrows), (D) a whale shark, *Rhincodon typus*, terminates directional travel with extensive turning to exploit a prey patch, (E) an Alpine ibex, *Capra ibex*, uses a zig-zag movement path to ascend a slope (cf. Redcliffe, Wilson, et al., 2025), thereby saving energy (Llobera & Sluckin, 2007) and (F) a Mediterranean mouflon, *Ovis gmelini musimon*, in the last few seconds of its life runs and turns in a vain bid to escape capture by a wolf, *Canis lupus* (Wilson et al., 2015). (G) Shows how the incidence and extent of turns varies as animals (here Magellanic penguins, *Spheniscus magellanicus*) move through an environmentally varied landscape (each track is derived from an individual bird). Landscape categorization (shown in G) is based on drone imagery processed via Structure-from-Motion in Agisoft Photoscan version 1.4.3. The beach landscape was decrypted by eye (characterized by steep pebble drop off), and the no-, low-, medium-, and high-vegetation density types were allocated based on estimates of pixel density per gridded cell (a proxy of shrubbery extent) with ~10 m × 10 m resolution. Boxplot (boxes encompass the 25%–75% interquartile range, horizontal bars reflect the median, and whiskers extend to 1.5 times the interquartile range) were constructed using the mean values per bird and vegetation type. Silhouette illustrations credit: Imran Razik.

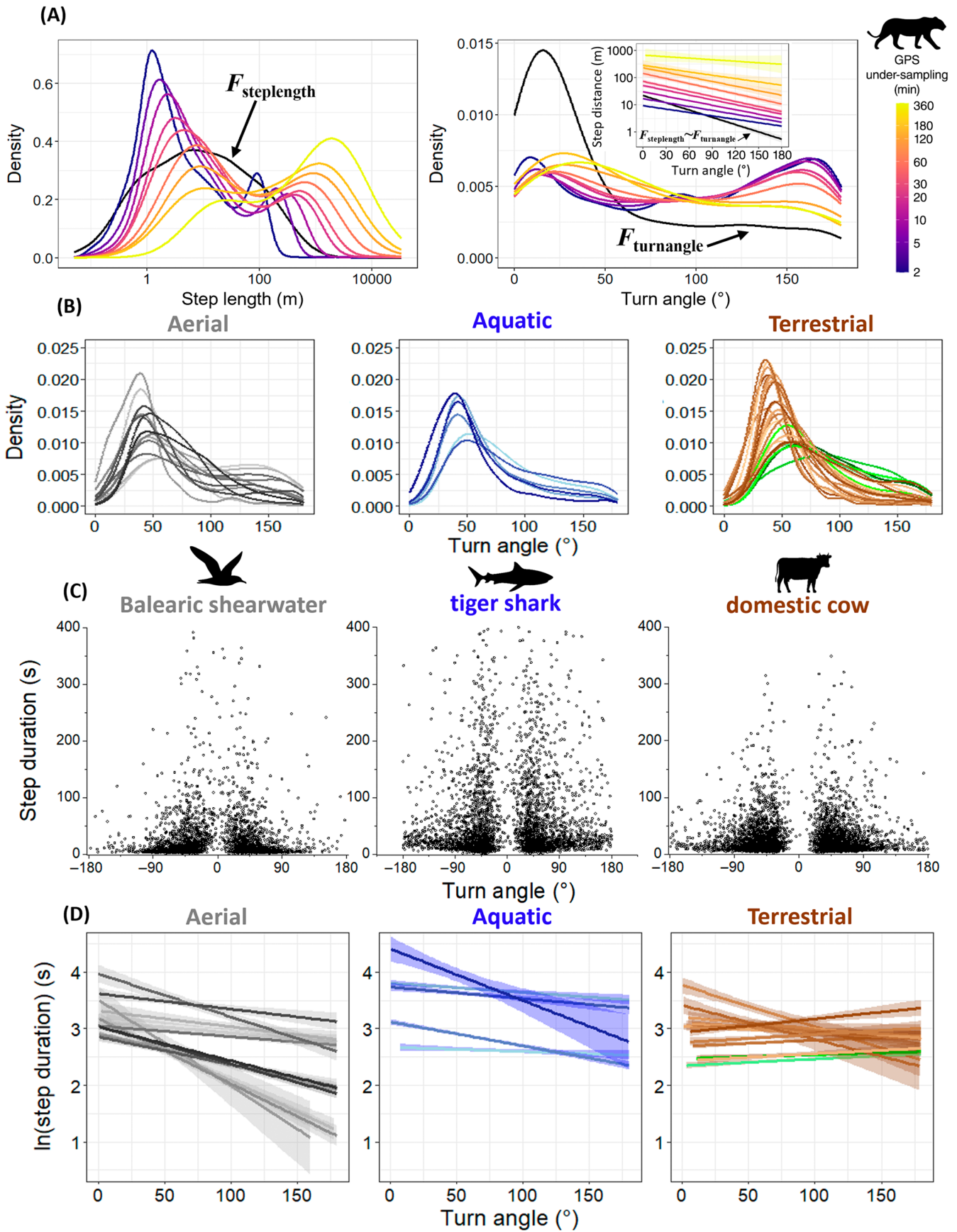


FIGURE 4 Legend on next page.

still show visual changes in turning-angle distributions over time, but our techniques were unable to distinguish these changes from those expected under uniform-random turning; the semiarborescent white-nosed coati, *Nasua narica*, also falls close to this boundary (Figure 5B).

We note also that the great frigatebird, *Fregata minor*, has the highest degree of straight-line wobble (Figure 1F) and the lowest proportion of straight-line travel of any of our species (Figure 1G). This species, along with the Andean condor, *Vultur gryphus*, is heavily dependent on local thermals and so must spend a substantial amount of time turning and gaining altitude within them.

Predicting animal movement

A vital aspect of understanding animal movement lies in our ability to predict animal paths under varying conditions, including future scenarios (Boult et al., 2018; Chudzinska et al., 2021). This requires the movement to be documented as a sequence of behavioral responses to spatially varying conditions. Our framework suggests that the interplay between $F_{\text{stepduration}}$ and $F_{\text{turnangle}}$ distributions reflects changes in traveling behavior and responses to particular spatial conditions (see Figure 3G). However, while these distributions provide valuable insights, they cannot on their own generate realistic movement paths due to the absence of overall directionality.

To address this, we developed an agent-based model (Railsback & Grimm, 2019) that integrates highly resolved empirical data to analyze the ability of our characterized $F_{\text{stepduration}}$ and $F_{\text{turnangle}}$ distributions to predict realistic paths of animal movement. By imposing general headings on projected movement path sectors, based on prior observations linking headings with $F_{\text{stepduration/length}}$ and $F_{\text{turnangle}}$ distributions, the model more closely resembles real movement trajectories. We illustrate this using Magellanic penguins foraging for their chicks. These penguins operate in open seas, with few physical obstacles and relatively low predation risk, so turning decisions are expected to be driven largely by prey

availability and navigation needs. Real data also reveal where prey are caught (Appendix S1: Section S5), enabling metrics for prey density to be allocated to specific spatial cells and linked to local distributions of $F_{\text{steplengths}}$, $F_{\text{turnangles}}$ and heading, thereby allowing predictions of foraging success.

Our time- and space-specific distributions of $F_{\text{steplengths}}$ and $F_{\text{turnangles}}$ used in our agent-based model produced closer alignment with patterns observed in actual penguin tracks and markedly higher prey harvesting rates than conventional animal movement models (correlated random walks and Lévy flights; Figure 6A,B). Importantly, changes in $F_{\text{steplength}}$ and $F_{\text{turnangle}}$ distributions in relation to prey density facilitate the prediction of movements under various “what if” scenarios. For example, altering prey densities across foraging areas (see Appendix S1: Section S5 for details) allows explicit predictions about the spatial extent the model birds will utilize (Figure 6C), with important implications for time and energy expenditure (Chudzinska et al., 2021).

Our proposal that agent-based models can utilize $F_{\text{stepdurations/lengths}}$ and $F_{\text{turnangles}}$ to predict animal movement can be further refined because $F_{\text{turnangles}}$ may reflect behavioral responses as animals move toward attractants or away from repellents (Gunner et al., 2023) (Figures 3G and 5A). Incorporating both incentive and repulsion mechanisms into models can enhance our understanding and prediction of how wild animals react to specific features such as roads (Shepard et al., 2008) or wind turbines (Pedersen & Poulsen, 1991). This approach may also aid in developing cues to guide animals away from known threats. In our increasingly human-perturbed world, such refinements are pivotal for assessing the consequences of conservation-oriented interventions, thereby contributing to species protection and persistence (Boult et al., 2018).

One promising field where agent-based models of animal behavior can make a significant contribution is the modeling of marine ecosystems (Irvine et al., 2025; van Putten et al., 2012). Marine ecosystem models (MEMs) are conceptual frameworks designed to capture the

FIGURE 4 Turning angles, step durations, and step lengths and their interrelationships depend on data acquisition protocols. (A) Frequency distribution of step distances and turn angles for African lions, *Panthera leo* as a function of the frequency with which the location data were collected (where we had high resolution GPS location data and could compare these to $F_{\text{steplength}}$ and $F_{\text{turnangle}}$ data [black lines]). The insert shows the best fit lines between $F_{\text{steplength}}$ and $F_{\text{turnangle}}$ juxtaposed with the GPS approach based on the level of under-sampling. (B) Frequency distribution of $F_{\text{turnangle}}$ for the 43 species examined during movement trajectories according to lifestyle, (C) examples of how $F_{\text{stepdurations}}$ relate to $F_{\text{turnangles}}$ in example aerial, aquatic, and terrestrial animals and (D) best fit lines between $F_{\text{stepduration}}$ and $F_{\text{turnangle}}$ for those species where the two parameters were significantly correlated ($p < 0.05$). The best fit lines are derived from linear models, and the shading around these regression lines represents the standard error. Note, in panels (A), (B), and (D), turn angles are presented as absolute values (ranging from 0° to 180°), and in panel (C), turn angles are signed (spanning from -180° to +180°). Silhouette illustrations credit: Imran Razik.

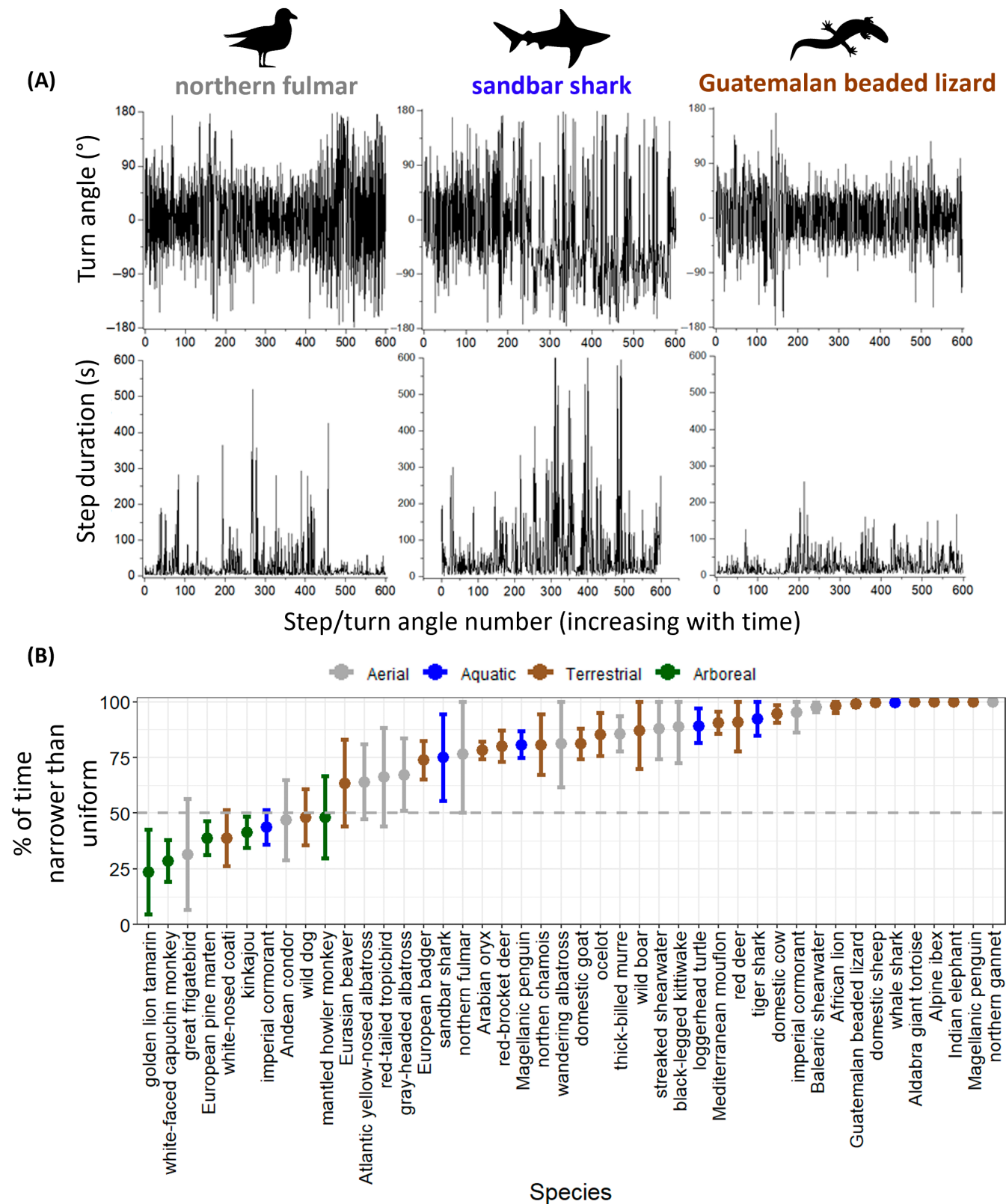


FIGURE 5 Fundamental step duration and fundamental turn-angle distributions vary over time. (A) Examples of changing distributions of $F_{\text{stepduration}}$ and $F_{\text{turnangles}}$ over time. Data consist of 600 sequential steps for three species representing aerial, aquatic, and terrestrial lifestyles/movement, showing how there are clear periods of time when the animals adopt particular step durations and/or particular turn angles. (B) The percentage of time that the animal's (local-in-time) turning angle distribution is narrower than that of a uniform distribution (see Appendix S1: Section S2 and Table S2 for methodological details). Silhouette illustrations credit: Imran Razik.

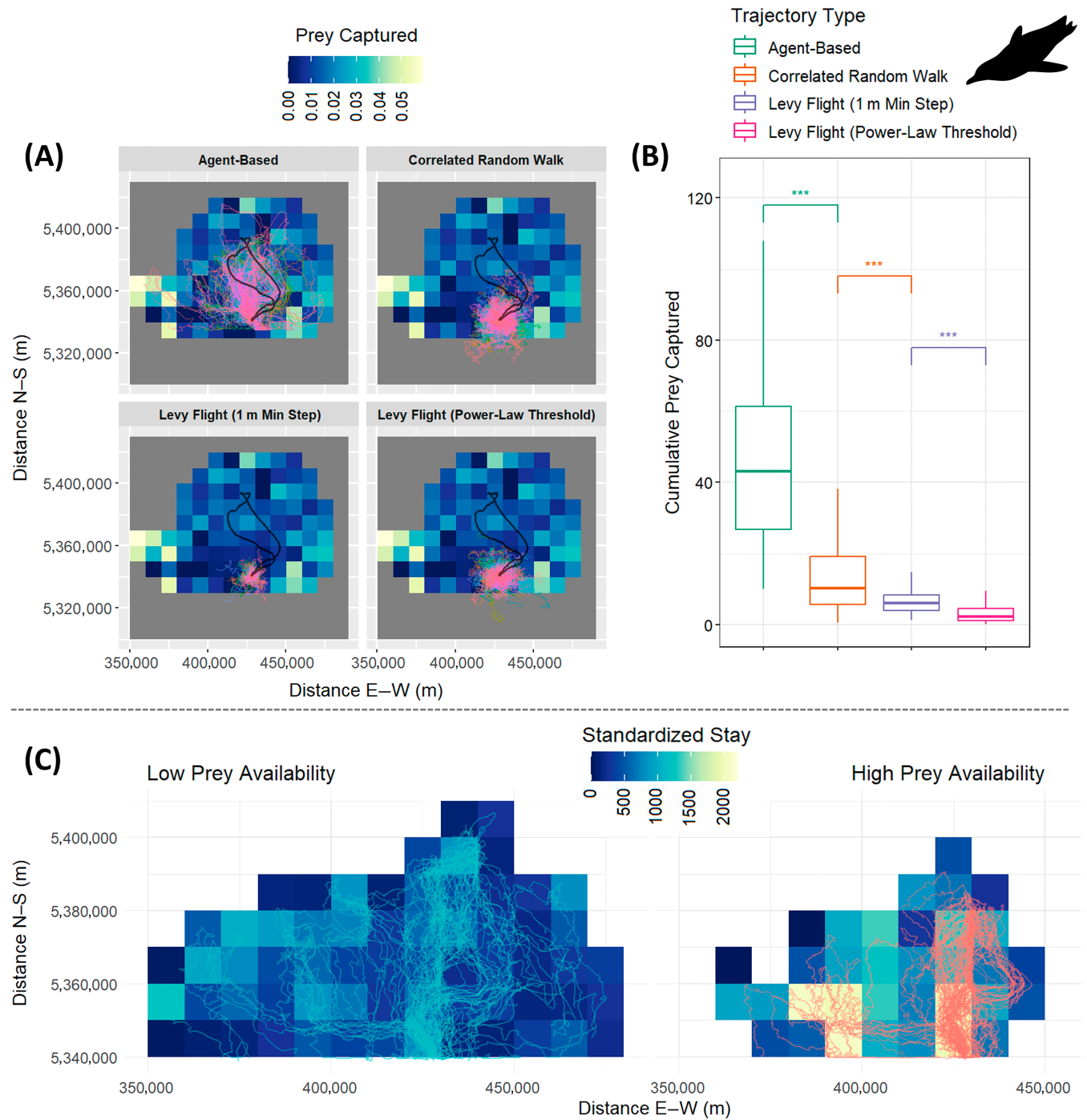


FIGURE 6 $F_{\text{steplength}}$ and $F_{\text{turnangles}}$ incorporating spatially linked heading information enhance predictions of animal movement paths. (A) The movement path of 300 agents simulating Magellanic penguins during single foraging trips from their breeding colony, compared to agents using correlated random walk and Lévy flight models. The black path represents an example of an actual penguin movement for comparison. (B) The predicted total number of prey items captured by each movement model used in (A). Boxes represent the interquartile range (25th–75th percentiles), horizontal bars indicate the median, and whiskers extend to 1.5 times the interquartile range. Asterisks denote significant pairwise differences ($p < 0.001$, Wilcoxon signed-rank tests). (C) Predicted foraging movements of 50 agents simulating penguins using $F_{\text{steplength}}$ and $F_{\text{turnangle}}$ based on two different simulated prey density distributions. Note that the low prey distribution results in reduced time spent per cell and a substantial increase in the overall area prospected. Silhouette illustrations credit: Imran Razik.

whole-of-system, nonlinear dynamics of interactions between species in complex food webs (Steenbeek et al., 2021). While increasingly prominent in policy and

decision-making, there are relatively few published examples of MEMs that implement and validate empirically grounded, behavior-based movement, and many

applications continue to rely on simplified movement rules. The incorporation of empirically grounded, behavior-based movement in these models would not only provide ecological realism but also enhance their capacity to test and refine scientific hypotheses across different environmental and management regimes. This has direct relevance for ecosystem-based fisheries management, marine spatial planning, and systematic conservation planning, where species' dynamic space use must be understood in order to inform decision-making.

We suggest that simulations based on fundamental steps and turns could be used to link event-scale movement to coarser sampled paths (Ruiz-Suarez et al., 2020) and clarify what “steps” represent in step-based models such as Step Selection Functions (SSFs). SSFs compare observed steps at a user-defined sampling interval to alternative (“available”) steps in relation to environmental covariates (Klappstein et al., 2024; Thurfjell et al., 2014). When multiple fundamental turns occur within an interval, the observed step is an aggregated outcome of several event-scale decisions, so SSF covariate signals may reflect both habitat selection and within-interval turn aliasing arising from aggregation of multiple event-scale decisions. Relatedly, Munden et al. (2021) present a turning-point-based SSF framework designed to align steps with behaviorally meaningful reorientation events when high-frequency data are available. Practically, high-frequency step/turn data can augment SSFs in three ways. First, event-based turning points can define behaviorally meaningful steps (turn-to-turn) at which habitat choice is evaluated, rather than imposing an arbitrary fixed interval. Second, empirically derived distributions of $F_{\text{stepdurations/lengths}}$ and $F_{\text{turnangles}}$ can be used to parameterize (or regularize) the availability kernel used to generate available steps, particularly for conventional SSFs, and for prediction/forward simulation in iSSFs where selection inference is, in principle, robust to the chosen kernel if it is correctly incorporated. Third, simulation approaches that embed event-scale step/turn processes but are then observed at coarser intervals provide a route to quantify (and potentially correct) sampling-induced bias in step/turn statistics and selection estimates (Ruiz-Suarez et al., 2020). At coarser sampling intervals (minutes to hours), the observed “steps” will generally not correspond to single fundamental steps but to net displacement after multiple turns, so apparent steps tend to be longer and paths may appear straighter than at event scale. Consequently, the “>90% straight-line travel” result should not be expected to hold in the same way when paths are reconstructed from sparse fixes: apparent straightness becomes a function of sampling interval and location error. In practice, this implies that SSF movement

kernels should be treated as sampling-rate-dependent summaries of an underlying event-scale process, rather than assumed invariant across sampling regimes (as also noted by Fieberg et al., 2021). We note that the analyses here used single continuous travel segments per individual (typically 5–36 h), shorter than the durations often used for habitat selection studies; extensions to longer horizons are discussed below (“Extending the framework to broader taxa, questions, and scales”).

Linking fundamental steps to environmental space, behavior, and energetics

The ability to document and quantify individual decision points along an animal's movement path enables the construction of “decision landscapes”: spatial representations that reflect the cognitive demands associated with navigating particular environments (e.g., Figure 7A, showing a penguin decision landscape). These landscapes may offer insights into the role of sensory systems in spatial navigation and how animals engage with their surroundings. For instance, increased turning frequency may indicate environmental constraint or complexity, such as navigating through cluttered or structured habitats (e.g., Figure 3C). In more open environments, where such constraints are minimal (as is the case in Figure 7), decision density could instead serve as a proxy for navigational challenge. However, decision density may also reflect spatial variation in resource availability (e.g., prey/forage density) or encounter rates, where frequent turning arises from intensified search and pursuit in profitable patches. This framework can be further extended by examining variation in decision density under different conditions, such as day versus night or in relation to proximity to landmarks (Quintana et al., 2022; Shiomi et al., 2019).

Because turning incurs energetic costs (Wilson, Rose, Metcalfe, et al., 2021), the spatial distribution of turning effort can be used to approximate a “power landscape”: a map of the energetic investment associated with directional changes across space (Figure 7B). This differs fundamentally from the concept of an “energy landscape,” where movement cost is shaped by the physical structure of the environment (Shepard et al., 2013). Instead, the power landscape captures the energy invested in turning decisions, which are likely subject to strong selective pressures. For example, animals may favor slow, low-cost directional adjustments in routine movement while searching for their prey, while reserving high-power, rapid turns for prey pursuit and capture (Figure 7C) or predator evasion. In diving and soaring taxa, many of

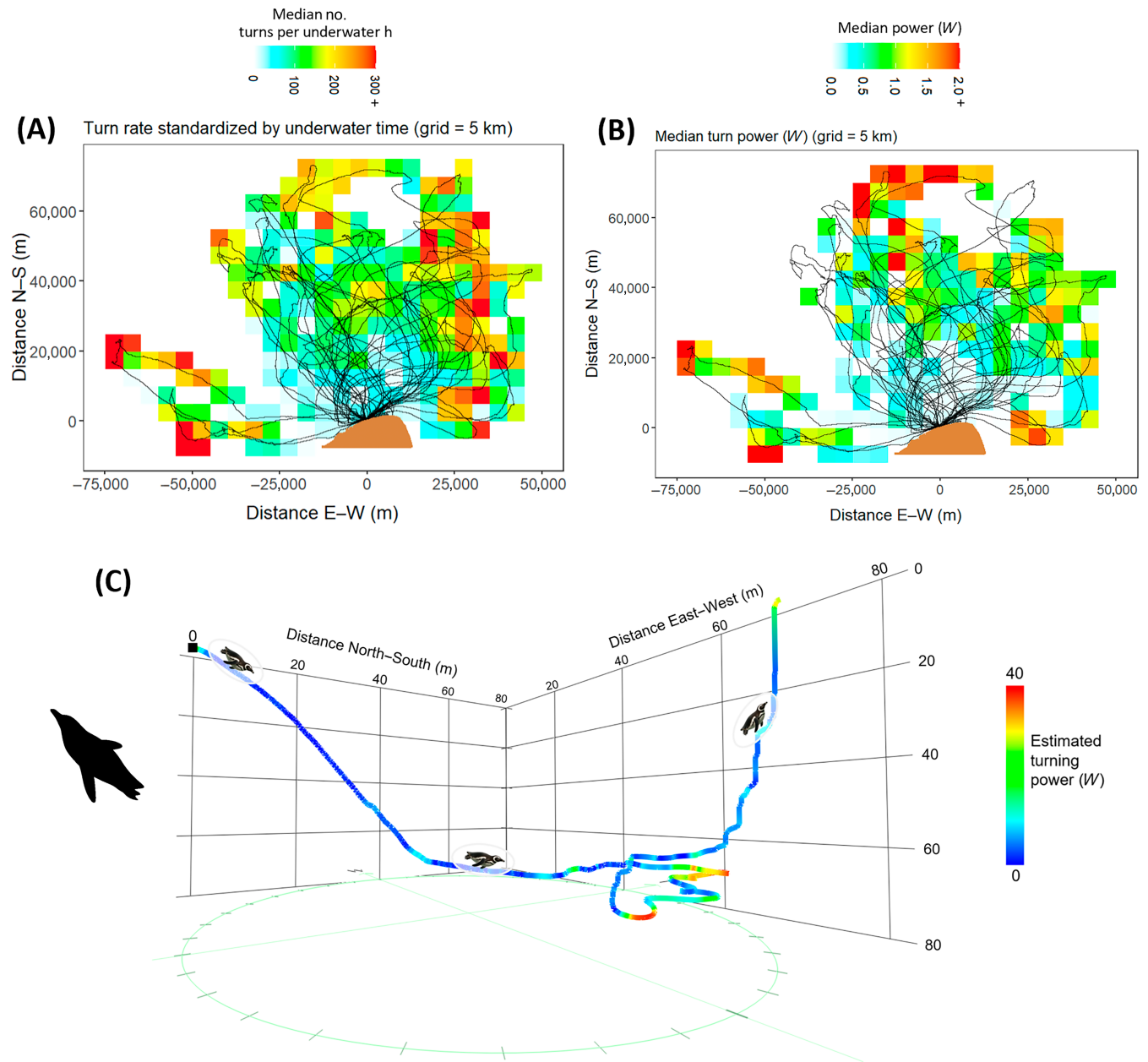


FIGURE 7 In open, obstacle-free pelagic water, Magellanic penguins exhibit heterogeneous decision- and power-based landscapes during foraging. (A) Heat map showing the spatial distribution of turning behavior (i.e., decision points—cf. Appendix S1: Section S2) by Magellanic penguins during foraging trips away from the colony (cf. Figure 6). Values reflect the median number of turns per hour underwater (cf. Appendix S1: Sections S2 and S4). Warmer colors denote higher turning frequency, notably higher at the outer limits of the foraging tracks, as would be expected in a central place foraging seabird (Ashmole, 1963; Elliott et al., 2009). (B) Turn-based “power landscape” calculated from the same tracks, based on the magnitude of the centripetal acceleration provided by the accelerometers during turning (Appendix S1: Section S4). The map shows the median across individuals but peak values could exceed 50 W. Cooler tones mark low turn power commuting corridors, whereas hot spots identify energetically costly zones due to high angular velocity turns during prey pursuit (cf. Ainley & Wilson, 2023). (C) Dead-reckoned path of a single example dive. The dive begins with long fundamental step lengths (royal blue sections) and shallow turn angles (cyan sections) as the bird homes in on prey, followed by tight, high-power turns (green to red sections) during pursuit. Together, the visualization shows that what is traditionally labeled “area-restricted search” appears to be a composite of distinct behaviors, here separated into area-restricted search versus area-restricted pursuit, each characterized by different fundamental turn-angle and step-length metrics. Silhouette illustrations credit: Imran Razik.

these decisions and energetic costs will also have a vertical component, motivating explicit 3D extensions of the framework.

By defining “fundamental steps” as periods of stable heading and “fundamental turning angles” as moments of active reorientation, our approach establishes a

mechanistic framework that directly links observable movement patterns to underlying biological processes. This conceptual shift transforms traditional descriptive analyses into hypothesis-driven investigations, enabling precise testing of how animals integrate sensory input, cognitive processes, and biomechanical constraints in response to ecological conditions. By grounding movement data in decision-making and effort allocation, this method offers predictive power for understanding animal behavior across contexts, from foraging and navigation to predator avoidance and habitat selection. Crucially, it opens new avenues for interpreting telemetry data with greater biological fidelity, offering a powerful tool for anticipating responses to environmental change, informing conservation strategies, and exploring the evolution of locomotor efficiency. Applied to large datasets encompassing multiple taxa, this framework represents a significant advance in movement ecology, enriching both theoretical understanding and applied ecological management.

Extending the framework to broader taxa, questions, and scales

Despite the generality of the “straight segments punctuated by turns” structure, extending the approach to a wider range of taxa and research questions depends on practical data constraints. The key requirement is sufficiently resolved directional information to detect reorientations at the time scale at which they occur. Magnetometer–accelerometer combinations enable this by providing tilt-compensated heading, but careful calibration, tag placement stability, and appropriate filtering are essential to minimize artifacts (e.g., local magnetic interference, changes in tag orientation, or motion-related noise) (Papafotis & Sotiriadis, 2020). Over broader spatial scales and longer deployments, additional considerations include geographic variation in magnetic inclination/declination and tag-related hard/soft-iron effects, which can bias heading if not accounted for (Ozyagcilar, 2012). These constraints, together with tag size and attachment limitations (cf. Wilson, Rose, Gunner, et al., 2021), mean that high-frequency inertial approaches will remain more feasible for some taxa and settings than others.

A second constraint is temporal coverage. Here we analyzed continuous segments (typically 5–36 h) to characterize fine-scale path structure and demonstrate cross-taxon regularities. For questions requiring longer horizons (e.g., diel routines, habitat selection, seasonal movements), the same framework can be extended by sampling multiple representative windows per individual

(e.g., repeated daily bouts), by duty-cycling high-frequency sensors, or by extracting and storing event-level summaries (e.g., turn times, step durations, turn magnitudes) rather than raw high-rate data (Williams, Taylor, et al., 2020). Where separating “travel” from “non-travel” states is important, inertial signatures (e.g., acceleration-based activity metrics) can be used to segment behavior prior to step/turn analysis (Qasem et al., 2012), while acknowledging that the most appropriate segmentation criteria may differ across locomotion modes (Gunner, Holton, Scantlebury, Hopkins, et al., 2021). More broadly, the metrics introduced here provide a bridge between high-frequency, event-based movement descriptions and coarser telemetry: They can inform how step-length and turn-angle distributions should be parameterized at lower sampling rates and help identify when coarse sampling is likely to alias multiple turns into single “steps,” thereby affecting inference in step-based and continuous-time models (Ruiz-Suarez et al., 2020).

Finally, extending this approach to fully three-dimensional trajectories requires integrating heading with pitch/roll and vertical movement (e.g., pressure/altitude), enabling turns to be defined in 3D and linked to volumetric environmental structure. Indeed, the turning-points algorithm of Potts et al. (2018) has been extended to 3D in such a way, for the purpose of detecting changes in head orientation of animals (Wilson et al., 2020). In the context of our study, this 3D extension is particularly relevant for aquatic and aerial taxa (e.g., Garde et al., 2023), where vertical maneuvers can be integral to prey pursuit and energy harvesting, and for arboreal movement where canopy connectivity and vertical stratification can constrain route choice and shape decision landscapes (Harel et al., 2022).

These extensions open the door to testing how route structure emerges from sensory range, environmental connectivity, and risk–reward trade-offs and to comparing how such mechanisms differ across habitats, locomotion modes, and individuals.

AUTHOR CONTRIBUTIONS

Conceptualization: Rory P. Wilson and Richard M. Gunner. Methodology: All authors. Investigation: Richard M. Gunner, Jonathan R. Potts, Rory P. Wilson, Miguel Lurgi, Juan M. Morales, James Redcliffe, Thomas Barbedette-Gerard, Mark D. Holton. Visualization: Richard M. Gunner, Jonathan R. Potts. Funding acquisition: Abdulaziz Alagaili, Bradley M. Norman, Carlos M. Duarte, David M. Scantlebury, Christophe Eizaguirre, Emily L. C. Shepard, Flavio Quintana, Frank Rosell, Henri Weimerskirch, Kyle H. Elliott, Ken Yoda, Luca Börger, Margaret C. Crofoot, Mark Meekan, Natasha Gillies, Peter

G. Ryan, Rory P. Wilson, Rebecca Scott, Sergio A. Lambertucci, Scott Creel, Vaclav Silovsky. Project administration: Rory P. Wilson, Richard M. Gunner. Writing—original draft: Rory P. Wilson, Richard M. Gunner. Writing—review and editing: all authors.

AFFILIATIONS

¹Department for the Ecology of Animal Societies, Max Planck Institute of Animal Behaviour, Konstanz, Germany

²Swansea Lab for Animal Movement, Department of Biosciences, Swansea University, Swansea, UK

³Centre for Biomathematics, Swansea University, Swansea, UK

⁴Department of Biology, University of Konstanz, Konstanz, Germany

⁵Smithsonian Tropical Research Institute, Balboa, Panama

⁶Department of Zoology, College of Science, King Saud University, Riyadh, Saudi Arabia

⁷Hopkins Marine Station, Stanford University, Pacific Grove, California, USA

⁸Centro de Estudios Ambientales y Biodiversidad, Universidad del Valle de Guatemala, Guatemala City, Guatemala

⁹Faculty of Technology, Natural Sciences and Maritime Sciences, Department of Natural Sciences and Environmental Health, University of South-Eastern Norway, Bø i Telemark, Norway

¹⁰École Normale Supérieure de Lyon, Université Claude Bernard Lyon 1, Université de Lyon, Lyon, France

¹¹Mammal Research Institute, Department of Zoology and Entomology, University of Pretoria, Pretoria, South Africa

¹²CEFE, Univ Montpellier, CNRS, EPHE, IRD, Montpellier, France

¹³College of Engineering, Swansea University, Swansea, UK

¹⁴Durrell Wildlife Conservation Trust, Les Augrès Manor, Jersey, UK

¹⁵Mauritian Wildlife Foundation, Vacoas, Mauritius

¹⁶Department of Ecology, Montana State University, Bozeman, Montana, USA

¹⁷Laboratório de Fisiologia Animal (LaFa), Departamento de Biodiversidade, UNESP, Rio Claro, São Paulo, Brazil

¹⁸Grupo de Investigaciones en Biología de la Conservación (GRINBIC), INIBIOMA (Universidad Nacional del Comahue-CONICET), Buenos Aires, Argentina

¹⁹Department of Game Management and Wildlife Biology, Faculty of Forestry and Wood Sciences, Czech University of Life Sciences, Prague, Czech Republic

²⁰Red Sea Research Centre, King Abdullah University of Science and Technology, Thuwal, Saudi Arabia

²¹School of Biological and Behavioural Sciences, Queen Mary University of London, London, UK

²²Department of Natural Resource Sciences, McGill University, Quebec, Canada

²³Office Français de la Biodiversité, Service Anthropisation et Fonctionnement des Ecosystèmes Terrestres, Gières, France

²⁴School of Environmental Sciences, University of Liverpool, Liverpool, UK

²⁵Department of Biology, University of Oxford, Oxford, UK

²⁶Centre for Sustainable Aquatic Ecosystems, Harry Butler Institute, Murdoch University, Murdoch, Western Australia, Australia

²⁷School of Biological Sciences, Queen's University Belfast, Belfast, UK

²⁸FitzPatrick Institute of African Ornithology, Department of Biological Sciences, University of Cape Town, Cape Town, South Africa

²⁹Diomedea Science – Research and Scientific Communication, Quaix-en-Chartreuse, France

³⁰School of Biological, Earth & Environmental Sciences, University College Cork, Cork, Ireland

³¹Departamento de Ecología, Genética y Evolución & Instituto de Ecología, Genética y Evolución de Buenos Aires (IEGEBA – CONICET - UBA), Facultad de Ciencias Exactas y Naturales, Universidad de Buenos Aires, Pabellón II, Ciudad Universitaria, Buenos Aires, Argentina

³²Max Planck Institute of Animal Behaviour, Radolfzell, Germany

³³Associação Mico-Leão-Dourado (AMLD), Silva Jardim, Rio de Janeiro, Brazil

³⁴Oceans Institute, University of Western Australia, Crawley, Western Australia, Australia

³⁵Ocean Sciences and Solutions Applied Research Institute, NEOM Corp, Gayal, Saudi Arabia

³⁶Graduate School of Environmental Studies, Nagoya University, Nagoya, Japan

³⁷Department of Ecoscience, Aarhus University, Aarhus C, Denmark

³⁸ECOCEAN Inc, Coogee, Western Australia, Australia

³⁹Harry Butler Institute, Murdoch University, Murdoch, Western Australia, Australia

⁴⁰IMBE, Aix Marseille Univ, Avignon Univ, CNRS, IRD, Marseille, France

⁴¹Ligue pour la Protection des Oiseaux, Pleumeur-Bodou, France

⁴²Green screen Festival e.V, Eckernförde, Germany

⁴³Instituto de Biología de Organismos Marinos (IBIOMAR), CONICET, Puerto Madryn, Argentina

⁴⁴Laboratório de Ciências Ambientais, Universidade Estadual do Norte Fluminense, Campos dos Goytacazes, Rio de Janeiro, Brazil

⁴⁵NERC, Polaris House, North Star Avenue, Swindon, UK

⁴⁶Ecopath International Initiative, Barcelona, Spain

⁴⁷Department of Fisheries, Wildlife, and Conservation Sciences, Oregon State University, Corvallis, Oregon, USA

⁴⁸Centre d'Etudes Biologiques de Chizé (CEBC), UMR 7372 CNRS-La Rochelle Université, Villiers-en-Bois, France

⁴⁹School of Biodiversity, One Health & Veterinary Medicine, University of Glasgow, Glasgow, UK

⁵⁰Grupo de Ecología Cuantitativa, INIBIOMA-CONICET, CRUB, San Carlos de Bariloche, Argentina

⁵¹School of Mathematical and Physical Sciences, University of Sheffield, Sheffield, UK

ACKNOWLEDGMENTS

Please refer to Appendix S1: Section S1 for specific acknowledgments, ethical approvals, and funding sources (in addition to those listed below) related to each species analyzed in this study. We thank Imran Razik, designer and science communicator (Department for the Ecology of Animal Societies, Max Planck Institute of Animal Behavior, Konstanz, Germany), for creating the silhouette illustrations. Sergio A. Lambertucci thanks Humboldt Foundation for support. This work was supported by Ailes Marines (David Grémillet), the Department for Economy Global Challenges Research Fund grant (David M. Scantlebury). The Beveridge Herpetological Trust, International Association of Avian Trainers & Educators (IAATE) and the ANCYPT grant PICT 2021-I-A-00484 (Sergio A. Lambertucci), by Durrell Conservation Trust; Supporting Project RSPD2023R602, from King Saud University, the Deanship of Scientific Research at the King Saud University through Vice Deanship of Research Chairs (Abdulaziz Alagaili), the Royal Society/Wolfson Lab refurbishment scheme (Rory P. Wilson), the Humboldt Foundation (Rory P. Wilson), the Royal Society for the Protection of Birds and the South African National Antarctic Programme (Peter G. Ryan), the Biotechnology and Biological Sciences Research Council (BBSRC), grant BB/M011224/1 (Natasha Gillies), the NSERC Discovery Grant and the European Research Council under the European Union's Horizon 2020 research and innovation program, grant 715874 (ELCS), the Argentine fund for scientific and technological research (FONCyT), grant PICT 2015 0815 (Juan M. Morales), the Department of Agriculture, Environment and Rural Affairs, Northern Ireland (David M. Scantlebury), the Royal Norwegian Society of Sciences

and Letters Special (Frank Rosell), the Challenge Fund and Newry, Mourne and Down District Council, the College of Science Santander Travel Grant, the European Research Council Advanced Grant under The European Research Council Advanced Grant Program FP7/2007–2013, grant no. ERC-2012-ADG_20120314 and European Union's Horizon Europe Research and Innovation Programme under grant agreement No. 101060072 (ACTNOW), the National Agency for Science Promotion, grant PICT 2018-01480 and PICT 2017-1996, under the aegis of the Ministerio de Ciencia, Tecnología e Innovación Productiva, Argentina (Flavio Quintana), the First Trust Travel Scholarship at Queen's University Belfast (Aoife Göppert), the Max Planck Institute for Animal Behaviour's Department for the Ecology of Animal Societies (directed by Margaret C. Crofoot), the Future Ocean Cluster of Excellence grant CP1217 (Rebecca Scott), the National Geographic grant GEFNE69-13 (Christophe Eizaguirre), the Whitley Wildlife Conservation Trust (Christophe Eizaguirre), the Future Ocean Capacity Building (Christophe Eizaguirre), the King Abdullah University of Science and Technology (KAUST) under the KAUST Sensor Initiative (led by Carlos M. Duarte), the European Regional Development fund through the Ireland Wales Co-operation Programme, the University Grant Competition at the Czech University of Life Sciences in Prague, grant 82/2021, the Ministry of Agriculture of the Czech Republic, the OP RDE project Improvement in Quality of the Internal Grant Scheme at CZ, grant CZ,02.2.69/0.0/0.0/19_073/0016944, the "EVA4.0" grant CZ,02.1.01/0.0/0.0/16_019/0000803 financed by OP RDE, and supported by "NAZV" grant QK1910462, the Crowdfunding campaign on the Experiment platform (<https://doi.org/10.18258/7190>), the Holsworth Wildlife Research Endowment, the UWA Graduate Research School for fieldwork, the Australian Institute of Marine Science, the Japan Society of the Promotion of Science through Grants-in-Aid for Scientific Research, grants 16H01769, 16H06541, 22H00569, 21H05294, the JST CREST grant JPMJCR23P2, Japan (Ken Yoda), the Estate of the late Winifred Violet Scott, the Jock Clough Marine Foundation, Rolex Awards for Enterprise (Rory P. Wilson, Bradley M. Norman), the MG Kailis Group (Bradley M. Norman), RAC Parks and Resorts (Bradley M. Norman), the National Science Foundation, grants IOS1145749 and DEB-2032131 (Scott Creel), the National Geographic Society Big Cats Initiative, the Gemfields Inc. World Wildlife Fund–Netherlands & Zambia, the Bennink Foundation, Painted Dog Conservation Inc. and Kayte Simpson, Prabha Sarangi and Connor Clairmont, Wilderness Wildlife Trust, Tusk Trust, Panthera, Elephant Charge, Ntengu Safaris, the IUCN Save Our Species/European Union, and the European Research Executive Agency (REA) for providing

support for the analysis (cross-species) Project 101060072 – ACTNOW. Open Access funding enabled and organized by Projekt DEAL.

CONFLICT OF INTEREST STATEMENT

The authors declare no conflicts of interest.

DATA AVAILABILITY STATEMENT

Data (Gunner et al., 2026) are available in Dryad at <https://doi.org/10.5061/dryad.gxd2547sd>. Code (Gunner, 2026) supporting the agent-based simulation is available in Zenodo at <https://doi.org/10.5281/zenodo.18909038>.

ORCID

Richard M. Gunner  <https://orcid.org/0000-0002-2054-9944>

Miguel Lurgi  <https://orcid.org/0000-0001-9891-895X>

Samantha Andrzejczek  <https://orcid.org/0000-0002-9929-7312>

Daniel Ariano-Sánchez  <https://orcid.org/0000-0003-4955-5018>

Scott Creel  <https://orcid.org/0000-0003-3170-6113>

Aoife Göppert  <https://orcid.org/0000-0002-9100-5717>

Sergio A. Lambertucci  <https://orcid.org/0000-0002-2624-2185>

Pascal Marchand  <https://orcid.org/0000-0002-0710-8861>

Mark Meekan  <https://orcid.org/0000-0002-3067-9427>

Rasmus M. Mortensen  <https://orcid.org/0000-0003-4975-608X>

Aurore Ponchon  <https://orcid.org/0000-0002-5126-6269>

Samantha D. Reynolds  <https://orcid.org/0000-0003-4094-8018>

Carlos R. Ruiz-Miranda  <https://orcid.org/0000-0001-7360-0304>

Joshua P. Twining  <https://orcid.org/0000-0002-0881-9665>

Ken Yoda  <https://orcid.org/0000-0002-8346-3291>

Henri Weimerskirch  <https://orcid.org/0000-0002-0457-586X>

Shannon Whelan  <https://orcid.org/0000-0003-2862-327X>

Juan M. Morales  <https://orcid.org/0000-0001-7269-7490>

Jonathan R. Potts  <https://orcid.org/0000-0002-8564-2904>

REFERENCES

- Ainley, D. G., and R. P. Wilson. 2023. *The Aquatic World of Penguins: Biology of Fish-Birds*. Cham: Springer.
- Alexander, R. M. N. 2003. *Principles of Animal Locomotion*. Princeton, NJ: Princeton University Press.
- Ashmole, N. P. 1963. "The Regulation of Numbers of Tropical Oceanic Birds." *Ibis* 103b: 458–473.
- Bailey, J. D., A. J. King, E. A. Codling, A. M. Short, G. I. Johns, and I. Fürtbauer. 2021. "'Micropersonality' Traits and Their Implications for Behavioral and Movement Ecology Research." *Ecology and Evolution* 11: 3264–73.
- Barraquand, F., and S. Benhamou. 2008. "Animal Movements in Heterogeneous Landscapes: Identifying Profitable Places and Homogeneous Movement Bouts." *Ecology* 89: 3336–48.
- Bartumeus, F., M. G. E. da Luz, G. M. Viswanathan, and J. Catalan. 2005. "Animal Search Strategies: A Quantitative Random-Walk Analysis." *Ecology* 86: 3078–87.
- Bidder, O. R., J. S. Walker, M. W. Jones, M. D. Holton, P. Urge, D. M. Scantlebury, N. J. Marks, E. A. Magowan, I. E. Maguire, and R. P. Wilson. 2015. "Step by Step: Reconstruction of Terrestrial Animal Movement Paths by Dead-Reckoning." *Movement Ecology* 3: 23.
- Biewener, A. A., and M. A. Daley. 2007. "Unsteady Locomotion: Integrating Muscle Function with Whole Body Dynamics and Neuromuscular Control." *Journal of Experimental Biology* 210: 2949–60.
- Boult, V. L., T. Quaife, V. Fishlock, C. J. Moss, P. C. Lee, and R. M. Sibly. 2018. "Individual-Based Modelling of Elephant Population Dynamics Using Remote Sensing to Estimate Food Availability." *Ecological Modelling* 387: 187–195.
- Brown, G. L., N. Seethapathi, and M. Srinivasan. 2021. "A Unified Energy-Optimality Criterion Predicts Human Navigation Paths and Speeds." *Proceedings of the National Academy of Sciences* 118: e2020327118.
- Calabrese, J. M., C. H. Fleming, and E. Gurarie. 2016. "Ctmm: An R Package for Analyzing Animal Relocation Data as a Continuous-Time Stochastic Process." *Methods in Ecology and Evolution* 7: 1124–32.
- Calabrese, J. M., C. H. Fleming, M. J. Noonan, and X. Dong. 2021. "Ctmmweb: A Graphical User Interface for Autocorrelation-Informed Home Range Estimation." *Wildlife Society Bulletin* 45: 162–69.
- Chudzinska, M., J. Nabe-Nielsen, S. Smout, G. Aarts, S. Brasseur, I. Graham, P. Thompson, and B. McConnell. 2021. "AgentSeal: Agent-Based Model Describing Movement of Marine Central-Place Foragers." *Ecological Modelling* 440: 109397.
- Costa, D. P., P. W. Robinson, J. P. Y. Arnould, A.-L. Harrison, S. E. Simmons, J. L. Hassrick, A. J. Hoskins, et al. 2010. "Accuracy of ARGOS Locations of Pinnipeds at-Sea Estimated Using Fastloc GPS." *PLoS One* 5: e8677.
- Dall, S. R., L.-A. Giraldeau, O. Olsson, J. M. McNamara, and D. W. Stephens. 2005. "Information and its Use by Animals in Evolutionary Ecology." *Trends in Ecology & Evolution* 20: 187–193.
- DeCesare, N. J., J. R. Squires, and J. A. Kolbe. 2005. "Effect of Forest Canopy on GPS-Based Movement Data." *Wildlife Society Bulletin* 33: 935–941.
- Dewhurst, O. P., H. K. Evans, K. Roskill, R. J. Harvey, T. Y. Hubel, and A. M. Wilson. 2016. "Improving the Accuracy of Estimates of Animal Path and Travel Distance Using GPS Drift-Corrected Dead Reckoning." *Ecology and Evolution* 6: 6210–22.
- Domenici, P. 2001. "The Scaling of Locomotor Performance in Predator–Prey Encounters: From Fish to Killer Whales."

- Comparative Biochemistry and Physiology Part A: Molecular & Integrative Physiology* 131: 169–182.
- Dorfman, A., T. T. Hills, and I. Scharf. 2022. “A Guide to Area-Restricted Search: A Foundational Foraging Behaviour.” *Biological Reviews* 97: 2076–89.
- Elliott, K. H., K. J. Woo, A. J. Gaston, S. Benvenuti, L. Dall’Antonia, and G. K. Davoren. 2009. “Central-Place Foraging in an Arctic Seabird Provides Evidence for Storer-Ashmole’s Halo.” *The Auk* 126: 613–625.
- Fagan, W. F., M. A. Lewis, M. Auger-Méthé, T. Avgar, S. Benhamou, G. Breed, L. LaDage, U. E. Schlägel, W. w. Tang, and Y. P. Papastamatiou. 2013. “Spatial Memory and Animal Movement.” *Ecology Letters* 16: 1316–29.
- Fernandez, P. A. 2014. “Reasoning and the Unity of Aristotle’s Account of Animal Motion.” *Oxford Studies in Ancient Philosophy* 47: 151–204.
- Fieberg, J., J. Signer, B. Smith, and T. Avgar. 2021. “A ‘How to’ Guide for Interpreting Parameters in Habitat-Selection Analyses.” *Journal of Animal Ecology* 90: 1027–43.
- Fleming, C. H., J. Drescher-Lehman, M. J. Noonan, T. S. B. Akre, D. J. Brown, M. M. Cochrane, N. Dejid, et al. 2020. “A Comprehensive Framework for Handling Location Error in Animal Tracking Data.” bioRxiv:2020.2006.2012.130195.
- Garde, B., A. Fell, K. Krishnan, C. G. Jones, R. Gunner, V. Tatayah, N. C. Cole, E. Lempidakis, and E. L. C. Shepard. 2023. “Thermal Soaring in Tropicbirds Suggests that Diverse Seabirds May Use this Strategy to Reduce Flight Costs.” *Marine Ecology Progress Series* 723: 171–183.
- Goodale, E., G. Beauchamp, R. D. Magrath, J. C. Nieh, and G. D. Ruxton. 2010. “Interspecific Information Transfer Influences Animal Community Structure.” *Trends in Ecology & Evolution* 25: 354–361.
- Gunner, R., R. Wilson, M. Lurgi, L. Börger, J. Redcliffe, E. Shepard, M. Holton, et al. 2026. “High Resolution Data Reveal Fundamental Steps and Turns in Animal Movements: Animal Heading Datasets.” Dryad [Dataset]. <https://doi.org/10.5061/dryad.gxd2547sd>
- Gunner, R. M. 2026. “Richard6195/Agent-Based_Fundamental_Steps_and_Turns_Simulation-: v1.0.0 – Gundog.sim Initial Public Release.” Zenodo [Software]. <https://doi.org/10.5281/zenodo.18909038>
- Gunner, R. M., M. D. Holton, D. M. Scantlebury, P. Hopkins, E. L. C. Shepard, A. J. Fell, B. Garde, et al. 2021. “How Often Should Dead-Reckoned Animal Movement Paths be Corrected for Drift?” *Animal Biotelemetry* 9: 43.
- Gunner, R. M., M. D. Holton, M. D. Scantlebury, O. L. van Schalkwyk, H. M. English, H. J. Williams, P. Hopkins, et al. 2021. “Dead-Reckoning Animal Movements in R: A Reappraisal Using Gundog.Tracks.” *Animal Biotelemetry* 9: 23.
- Gunner, R. M., R. P. Wilson, M. D. Holton, N. C. Bennett, A. N. Alagaili, M. F. Bertelsen, O. B. Mohammed, et al. 2023. “Examination of Head Versus Body Heading May Help Clarify the Extent to which Animal Movement Pathways Are Structured by Environmental Cues?” *Movement Ecology* 11: 71.
- Gunner, R. M., R. P. Wilson, M. D. Holton, P. Hopkins, S. H. Bell, N. J. Marks, N. C. Bennett, et al. 2022. “Decision Rules for Determining Terrestrial Movement and the Consequences for Filtering High-Resolution Global Positioning System Tracks: A Case Study Using the African Lion (*Panthera leo*).” *Journal of the Royal Society Interface* 19: 20210692.
- Gurarie, E., C. H. Fleming, W. F. Fagan, K. L. Laidre, J. Hernández-Pliego, and O. Ovaskainen. 2017. “Correlated Velocity Models as a Fundamental Unit of Animal Movement: Synthesis and Applications.” *Movement Ecology* 5: 13.
- Harel, R., S. Alavi, A. M. Ashbury, J. Aurisano, T. Berger-Wolf, G. H. Davis, B. T. Hirsch, et al. 2022. “Life in 2.5D: Animal Movement in the Trees.” *Frontiers in Ecology and Evolution* 10: 801850.
- Hills, T. T. 2006. “Animal Foraging and the Evolution of Goal-Directed Cognition.” *Cognitive Science* 30: 3–41.
- Hodel, F. H., and J. R. Fieberg. 2022. “Circular–Linear Copulae for Animal Movement Data.” *Methods in Ecology and Evolution* 13: 1001–13.
- Hooten, M. B., D. S. Johnson, B. T. McClintock, and J. M. Morales. 2017. *Animal Movement: Statistical Models for Telemetry Data*. Boca Raton, FL: CRC press.
- Humphries, N. E., N. Queiroz, J. R. M. Dyer, N. G. Pade, M. K. Musyl, K. M. Schaefer, D. W. Fuller, et al. 2010. “Environmental Context Explains Lévy and Brownian Movement Patterns of Marine Predators.” *Nature* 465: 1066–69.
- Hurford, A. 2009. “GPS Measurement Error Gives Rise to Spurious 180° Turning Angles and Strong Directional Biases in Animal Movement Data.” *PLoS One* 4: e5632.
- Irvine, L. M., B. A. Lagerquist, G. S. Schorr, E. A. Falcone, B. R. Mate, and D. M. Palacios. 2025. “Ecological Drivers of Movement for Two Sympatric Marine Predators in the California Current Large Marine Ecosystem.” *Movement Ecology* 13: 19.
- Johnson, D. S., J. M. London, M.-A. Lea, and J. W. Durban. 2008. “Continuous-Time Correlated Random Walk Model for Animal Telemetry Data.” *Ecology* 89: 1208–15.
- Kareiva, P., and G. Odell. 1987. “Swarms of Predators Exhibit ‘Preytaxis’ If Individual Predators Use Area-Restricted Search.” *The American Naturalist* 130: 233–270.
- Kashetsky, T., T. Avgar, and R. Dukas. 2021. “The Cognitive Ecology of Animal Movement: Evidence from Birds and Mammals.” *Frontiers in Ecology and Evolution* 9: 724887.
- Kays, R., M. C. Crofoot, W. Jetz, and M. Wikelski. 2015. “Terrestrial Animal Tracking as an Eye on Life and Planet.” *Science* 348: aaa2478.
- Kempton, J. A., J. Wynn, S. Bond, J. Evry, A. L. Fayet, N. Gillies, T. Guilford, et al. 2022. “Optimization of Dynamic Soaring in a Flap-Gliding Seabird Affects its Large-Scale Distribution at Sea.” *Science Advances* 8: eabo0200.
- Klappstein, N. J., T. Michelot, J. Fieberg, E. J. Pedersen, and J. Mills Flemming. 2024. “Step Selection Functions with Non-linear and Random Effects.” *Methods in Ecology and Evolution* 15: 1332–46.
- Llobera, M., and T. J. Sluckin. 2007. “Zigzagging: Theoretical Insights on Climbing Strategies.” *Journal of Theoretical Biology* 249: 206–217.
- McClintock, B. T., D. S. Johnson, M. B. Hooten, J. M. Ver Hoef, and J. M. Morales. 2014. “When to be Discrete: The Importance of Time Formulation in Understanding Animal Movement.” *Movement Ecology* 2: 21.
- Morales, J. M., D. T. Haydon, J. Frair, K. E. Holsinger, and J. M. Fryxell. 2004. “Extracting More out of Relocation Data: Building Movement Models as Mixtures of Random Walks.” *Ecology* 85: 2436–45.
- Morales, J. M., P. R. Moorcroft, J. Matthiopoulos, J. L. Frair, J. G. Kie, R. A. Powell, E. H. Merrill, and D. T. Haydon. 2010.

- “Building the Bridge between Animal Movement and Population Dynamics.” *Philosophical Transactions of the Royal Society B: Biological Sciences* 365: 2289–2301.
- Mueller, T., and W. F. Fagan. 2008. “Search and Navigation in Dynamic Environments—From Individual Behaviors to Population Distributions.” *Oikos* 117: 654–664.
- Munden, R., L. Börger, R. P. Wilson, J. Redcliffe, R. Brown, M. Garel, and J. R. Potts. 2021. “Why Did the Animal Turn? Time-Varying Step Selection Analysis for Inference between Observed Turning-Points in High Frequency Data.” *Methods in Ecology and Evolution* 12: 921–932.
- Nathan, R., W. M. Getz, E. Revilla, M. Holyoak, R. Kadmon, D. Saltz, and P. E. Smouse. 2008. “A Movement Ecology Paradigm for Unifying Organismal Movement Research.” *Proceedings of the National Academy of Sciences* 105: 19052–59.
- Nathan, R., C. T. Monk, R. Arlinghaus, T. Adam, J. Alós, M. Assaf, H. Baktoft, et al. 2022. “Big-Data Approaches Lead to an Increased Understanding of the Ecology of Animal Movement.” *Science* 375: eabg1780.
- Nolet, B. A., and W. M. Mooij. 2002. “Search Paths of Swans Foraging on Spatially Autocorrelated Tubers.” *Journal of Animal Ecology* 71: 451–462.
- Noonan, M. J., C. H. Fleming, T. S. Akre, J. Drescher-Lehman, E. Gurarie, A.-L. Harrison, R. Kays, and J. M. Calabrese. 2019. “Scale-Insensitive Estimation of Speed and Distance Traveled from Animal Tracking Data.” *Movement Ecology* 7: 35.
- Ozyagcilar, T. 2012. “Implementing a Tilt-Compensated eCompass Using Accelerometer and Magnetometer Sensors.” Freescale semiconductor, Application Note AN4248: Austin, TX.
- Papafotis, K., and P. P. Sotiriadis. 2020. “Accelerometer and Magnetometer Joint Calibration and Axes Alignment.” *Technologies* 8: 11.
- Pedersen, M., and E. Poulsen. 1991. “Avian Response to the Implementation of the Tjaereborg Wind Turbine at the Danish Wadden Sea.” *Danske Vildtundersoegelser* (Denmark).
- Plass, J. L., R. Moreno, and R. Brünken. 2010. *Cognitive Load Theory*. Cambridge: Cambridge University Press.
- Potts, J. R., L. Börger, D. M. Scantlebury, N. C. Bennett, A. Alagaili, and R. P. Wilson. 2018. “Finding Turning-Points in Ultra-High-Resolution Animal Movement Data.” *Methods in Ecology and Evolution* 9: 2091–2101.
- Proekt, A., J. R. Banavar, A. Maritan, and D. W. Pfaff. 2012. “Scale Invariance in the Dynamics of Spontaneous Behavior.” *Proceedings of the National Academy of Sciences* 109: 10564–69.
- Qasem, L., A. Cardew, A. Wilson, I. Griffiths, L. G. Halsey, E. L. C. Shepard, A. C. Gleiss, and R. Wilson. 2012. “Tri-Axial Dynamic Acceleration as a Proxy for Animal Energy Expenditure; Should We Be Summing Values or Calculating the Vector?” *PLoS One* 7: e31187.
- Quintana, F., A. Gómez-Laich, R. M. Gunner, F. Gabelli, G. D. Omo, C. Duarte, M. Brogger, and R. P. Wilson. 2022. “Long Walk Home: Magellanic Penguins Have Strategies That Lead Them to Areas Where They Can Navigate most Efficiently.” *Proceedings of the Royal Society B: Biological Sciences* 289: 20220535.
- Railsback, S. F., and V. Grimm. 2019. *Agent-Based and Individual-Based Modeling: A Practical Introduction*, Second ed. Princeton, NJ: Princeton University Press.
- Redcliffe, J., J. Boulerice, I. Namir, R. Wilson, W. J. McShea, and H. Shamon. 2025. “Using Dead-Reckoning to Track Movements and Map Burrows of Fossorial Species.” *Animal Biotelemetry* 13: 11.
- Redcliffe, J., R. Wilson, M. Holton, P. Hopkins, M. Garel, P. Marchand, G. Wilson, R. Brown, and L. Börger. 2025. “Steep Slopes, Shallow Angles: Mountain Ungulates Create their Own Topography through Movements.” *Canadian Journal of Zoology* 103: 1–18.
- Ruiz-Suarez, S., V. Leos-Barajas, I. Alvarez-Castro, and J. M. Morales. 2020. “Using Approximate Bayesian Inference for a ‘Steps and Turns’ Continuous-Time Random Walk Observed at Regular Time Intervals.” *PeerJ* 8: e8452.
- Shepard, D. B., A. R. Kuhns, M. J. Dreslik, and C. A. Phillips. 2008. “Roads as Barriers to Animal Movement in Fragmented Landscapes.” *Animal Conservation* 11: 288–296.
- Shepard, E. L., R. P. Wilson, W. G. Rees, E. Grundy, S. A. Lambertucci, and S. B. Vosper. 2013. “Energy Landscapes Shape Animal Movement Ecology.” *The American Naturalist* 182: 298–312.
- Shiomi, K., K. Sato, N. Katsumata, and K. Yoda. 2019. “Temporal and Spatial Determinants of Route Selection in Homing Seabirds.” *Behaviour* 156: 1165–83.
- Steenbeek, J., J. Buszowski, D. Chagaris, V. Christensen, M. Coll, E. A. Fulton, S. Katsanevakis, et al. 2021. “Making Spatial-Temporal Marine Ecosystem Modelling Better – A Perspective.” *Environmental Modelling & Software* 145: 105209.
- Thurfjell, H., S. Ciuti, and M. S. Boyce. 2014. “Applications of Step-Selection Functions in Ecology and Conservation.” *Movement Ecology* 2: 4.
- Turchin, P. 1998. *Quantitative Analysis of Movement: Measuring and Modeling Population Redistribution in Animals and Plants*. Sunderland, MA: Sinauer Associates.
- van Putten, I. E., R. J. Gorton, E. A. Fulton, and O. Thebaud. 2012. “The Role of Behavioural Flexibility in a Whole of Ecosystem Model.” *ICES Journal of Marine Science* 70: 150–163.
- Vickers, N. J. 2000. “Mechanisms of Animal Navigation in Odor Plumes.” *The Biological Bulletin* 198: 203–212.
- Voigt, C. C., and M. W. Holderied. 2012. “High Manoeuvring Costs Force Narrow-Winged Molossid Bats to Forage in Open Space.” *Journal of Comparative Physiology B* 182: 415–424.
- Weihs, D., and P. W. Webb. 1984. “Optimal Avoidance and Evasion Tactics in Predator-Prey Interactions.” *Journal of Theoretical Biology* 106: 189–206.
- Weimerskirch, H., D. Pinaud, F. Pawlowski, and C.-A. Bost. 2007. “Does Prey Capture Induce Area-Restricted Search? A Fine-Scale Study Using GPS in a Marine Predator, the Wandering Albatross.” *The American Naturalist* 170: 734–743.
- Williams, H. J., E. Shepard, M. D. Holton, P. Alarcón, R. Wilson, and S. Lambertucci. 2020. “Physical Limits of Flight Performance in the Heaviest Soaring Bird.” *Proceedings of the National Academy of Sciences* 117: 17884–90.
- Williams, H. J., L. A. Taylor, S. Benhamou, A. I. Bijleveld, T. A. Clay, S. de Grissac, U. Demšar, et al. 2020. “Optimizing the Use of Biologgers for Movement Ecology Research.” *Journal of Animal Ecology* 89: 186–206.
- Wilson, R., I. Griffiths, P. Legg, M. Friswell, O. Bidder, L. Halsey, S. A. Lambertucci, and E. Shepard. 2013. “Turn Costs Change the Value of Animal Search Paths.” *Ecology Letters* 16: 1145–50.
- Wilson, R. P., I. W. Griffiths, M. G. Mills, C. Carbone, J. W. Wilson, and D. M. Scantlebury. 2015. “Mass Enhances Speed but

Diminishes Turn Capacity in Terrestrial Pursuit Predators.” *eLife* 4: e06487.

- Wilson, R. P., K. A. Rose, R. Gunner, M. D. Holton, N. J. Marks, N. C. Bennett, S. H. Bell, et al. 2021. “Animal Lifestyle Affects Acceptable Mass Limits for Attached Tags.” *Proceedings of the Royal Society B: Biological Sciences* 288: 20212005.
- Wilson, R. P., K. A. Rose, R. S. Metcalfe, M. D. Holton, J. Redcliffe, R. Gunner, L. Börger, A. Loison, M. Jezek, and M. S. Painter. 2021. “Path Tortuosity Changes the Transport Cost Paradigm in Terrestrial Animals.” *Ecography* 44: 1524–32.
- Wilson, R. P., E. Shepard, and N. Liebsch. 2008. “Prying into the Intimate Details of Animal Lives: Use of a Daily Diary on Animals.” *Endangered Species Research* 4: 123–137.
- Wilson, R. P., H. J. Williams, M. D. Holton, A. di Virgilio, L. Börger, J. R. Potts, R. Gunner, et al. 2020. “An ‘Orientation Sphere’ Visualization for Examining Animal Head Movements.” *Ecology and Evolution* 10: 4291–4302.

SUPPORTING INFORMATION

Additional supporting information can be found online in the Supporting Information section at the end of this article.

How to cite this article: Gunner, Richard M., Rory P. Wilson, Miguel Lurgi, Luca Börger, James Redcliffe, Emily L. C. Shepard, Mark D. Holton, et al. 2026. “High Resolution Data Reveal Fundamental Steps and Turns in Animal Movements.” *Ecological Monographs* 96(2): e70069. <https://doi.org/10.1002/ecm.70069>